

Model Reduction and Clusterization of Large-Scale Bidirectional Networks

Takayuki Ishizaki, *Member, IEEE*, Kenji Kashima, *Member, IEEE*, Jun-ichi Imura, *Member, IEEE*,
Kazuyuki Aihara

Abstract—This paper proposes two model reduction methods for large-scale bidirectional networks that fully utilize a network structure transformation implemented as positive tridiagonalization. First, we present a Krylov-based model reduction method that guarantees a specified error precision in terms of the \mathcal{H}_∞ -norm. Positive tridiagonalization allows us to derive an approximation error bound for the input-to-state model reduction without computationally expensive operations such as matrix factorization. Second, we propose a novel model reduction method that preserves network topology among clusters, i.e., node sets. In this approach, we introduce the notion of cluster uncontrollability based on positive tridiagonalization, and then derive its theoretical relation to the approximation error. This error analysis enables us to construct clusters that can be aggregated with a small approximation error. The efficiency of both methods is verified through numerical examples, including a large-scale complex network.

Index Terms—Model Reduction, Network Systems, Network Clustering, Krylov Projection Method.

I. INTRODUCTION

DYNAMICAL systems over large-scale complex networks (large-scale dynamical networks), whose behaviors are described by an interaction of a large number of subsystems interconnected over a network, have been widely studied over the past decades. Examples of such dynamical networks include social networks, biological networks, power networks, and contagion networks (see [1], [2], [3], [4] for an overview). In general, their large-scale complexity makes straightforward application of the standard analysis and control synthesis methods very difficult. Thus, model reduction techniques become increasingly important as means of analysis and control synthesis (see [5], [6], [7] for a general overview).

For linear systems, various model reduction methods such as the balanced truncation [8], [9] and the Hankel norm approximation [10] have been extensively investigated, in which a bound of the approximation error in terms of, e.g., the \mathcal{H}_2 -, \mathcal{H}_∞ -, or Hankel norm is available (see [5], [11], [12], [13]). Actually, these methods generate a reduced order model conforming to a specified error precision through a systematic procedure. However, they are not necessarily

appropriate for the reduction of large-scale systems. This is because they require computationally expensive operations such as matrix factorization. Alternatively, moment matching methods [14], [15], [16], including the Krylov projection methods [5], [17], [18], [19], which suppress the discrepancy of the frequency response for specific input signals, have been developed toward the reduction of large-scale systems. However, even though these methods can be implemented by computationally efficient procedures, a priori error bounds have not yet been derived, except for the optimal \mathcal{H}_2 -reduction procedure established in the past few years [20].

The application of the aforementioned model reduction methods to large-scale dynamical networks raises a further consideration; the connection structure among subsystems is completely lost through the reduction. In other words, the application of such traditional methods extinguishes the physical meaning of subsystem state variables. More specifically, each state of the reduced model is obtained, in general, by a linear combination of all the original states. This limits the use of the reduced order model when one addresses, e.g., the distributed control problem and the sensor allocation problem. Hence, for large-scale dynamical networks, it is important to develop a *network topology-preserving* model reduction method, in which the projection matrix for reduction has some sparse structure to preserve a kind of network topology. To this end, we are required to deal with the following three challenges: (i) determining a set of subsystems, called a set of clusters, (ii) deriving a reduced order model compatible with the determined cluster set, and (iii) finding an error bound without direct use of the original model. Moreover, the implementation needs to be computationally efficient, for aiming at the reduction of large-scale systems.

As one possible approach to this kind of structured model reduction, [7] proposed a Krylov-based model reduction method for interconnected systems, in which the Krylov projection of each subsystem is considered to preserve the interconnection structure among the subsystems. However, this method not only requires a priori knowledge of the decomposition of the whole system into subsystems, but also provides no error evaluation. In a similar way, [12] proposed a structured balanced truncation method for interconnected systems in which the balanced truncation is applied to each subsystem, and [21] addressed a problem of clustering subsystems in the structured balanced truncation. However, they did not theoretically discuss the relation between the subsystem clustering and the resultant approximation error.

As related approaches, structure-preserving model reduc-

T. Ishizaki and J. Imura are with Graduate School of Information Science and Engineering, Tokyo Institute of Technology, 2-12-1, Meguro ward, Tokyo, Japan e-mail: {ishizaki, imura}@mei.titech.ac.jp.

K. Kashima is with Graduate School of Engineering Science, Osaka University, 1-3, Machikaneyama, Toyonaka, Osaka, Japan e-mail: kashima@sys.es.osaka-u.ac.jp

K. Aihara is with Institute of Industrial Science, University of Tokyo, 4-6-1 Komaba, Meguro ward, Tokyo, Japan e-mail: aihara@sat.t.u-tokyo.ac.jp.

Manuscript received June 27, 2011; revised April 6, 2012.

tion methods, e.g., [22], [23], [24], and state aggregation-based singular perturbation methods, e.g., [25], [26], [27], have been intensively investigated. In the former methods, reduced models are derived based on the Krylov projection for preserving the underlying structures of systems, such as the Lagrangian structure and the second-order structure, but not the network topology. The latter methods provide some theoretical relation between the approximation error and the strength of interconnection among subsystems. However, the singular perturbation approaches do not explicitly take into account the effect of the external input. In [28], the authors investigated the controllability of single-input networks from the point of view of graph theory, but they dealt with only a class of homogeneously interconnected networks. In addition, a state aggregation-based model reduction was proposed in [29]. However, no error analysis was carried out.

In contrast to these existing approaches, we propose two kinds of model reduction methods based on positive tridiagonalization, focusing on a class of large-scale bidirectional networks having a symmetric system matrix. First, we develop a Krylov-based model reduction method that guarantees a specified error precision. Our approach uses a concept of network structure transformation called positive tridiagonalization, which clarifies error analysis for a class of Krylov projection methods in terms of the \mathcal{H}_∞ -norm. It should be emphasized that the positive tridiagonalization is not utilized in the standard Krylov projection methods and this approach gives a further possibility for the error evaluation of those methods. Second, on the basis of the first method, we propose a novel clustering-based state aggregation procedure as one of the model reduction methods that preserve network topology among clusters, where network clustering, i.e., decomposition of the whole system into subsystems, is implemented in a systematic manner. By aggregating the states of the constructed clusters into lower-dimensional ones, we obtain an aggregated model that preserves the connection topology among the clusters.

During this clustering-based state aggregation, we first introduce a notion of cluster reducibility, which means that the state variables contained in a cluster have similar behavior for an arbitrary input signal, and then characterize the cluster reducibility by means of positive tridiagonalization. Next, we derive a qualitative relation between this reducibility and the aggregation error of the input-to-state transfer function, which allows us to use the reducibility as a design criterion for reduction. Finally, we show that the aggregation error can be evaluated by using the Krylov-based model reduction method proposed in the former part of the paper. This approach allows us to find a suitable cluster set in a systematic manner, without requiring a priori knowledge of the decomposition of the whole system into subsystems. It should be emphasized that our clustering approach is completely different from the existing ones in the sense that, fully utilizing the positive tridiagonalization, we introduce an index for clustering that is theoretically related to the resultant approximation error. Furthermore, owing to the numerical efficiency of tridiagonalization, our methods are applicable to large-scale bidirectional networks. Preliminary versions of this paper are found in [30],

[31], [32], [33].

The rest of this paper is organized as follows. In Section II, we describe the bidirectional network under investigation and define positive tridiagonalization for that bidirectional network. In Section III, based on the positive tridiagonalization, we propose the systematic procedure of a Krylov-based model reduction method that guarantees a specified error precision. In the last part of the section, the efficiency of the theoretical results is verified through a numerical example of a complex network with 3000 nodes and 6000 edges. In Section IV, we formulate a clustering-based state aggregation problem and provide a solution by fully exploiting the properties of the positive tridiagonalization. Furthermore, numerical examples including a complex network show that the proposed method is efficient. Concluding remarks are provided in Section V.

NOTATION: The following notation is used in this paper:

\mathbb{R}	set of real numbers
\mathbb{R}_+	set of nonnegative real numbers
I_n	unit matrix of size $n \times n$
e_i^n	i th column vector of I_n
$e_{i_1:i_2}^n$	i_1 th to i_2 th columns of I_n
$ \mathcal{I} $	cardinality of a set \mathcal{I}
$\ M\ $	l_2 -induced norm of a matrix M , i.e., maximum singular value of M
$\ M\ _{l_\infty}$	l_∞ -induced norm of a matrix $M = \{m_{i,j}\}$, i.e., $\max_i \sum_j m_{i,j} $
$\lambda_{\max}(M)$	maximum eigenvalue of a symmetric matrix M
$\lambda_{\min}(M)$	minimum eigenvalue of a symmetric matrix M
$\text{diag}(v)$	diagonal matrix having a vector v on its diagonal
$\text{Diag}(M_1, \dots, M_n)$	block diagonal matrix having matrices M_1, \dots, M_n on its block diagonal

The \mathcal{H}_∞ -norm of a stable rational transfer matrix G is defined by

$$\|G(s)\|_{\mathcal{H}_\infty} := \sup_{\omega \in \mathbb{R}} \|G(j\omega)\|.$$

For a set $\mathcal{I} \subseteq \{1, \dots, n\}$, $e_{\mathcal{I}}^n \in \mathbb{R}^{n \times |\mathcal{I}|}$ denotes the matrix whose column vectors are composed of e_i^n for each $i \in \mathcal{I}$ (in some order of i), i.e., $e_{\mathcal{I}}^n = [e_{i_1}^n, \dots, e_{i_m}^n] \in \mathbb{R}^{n \times m}$ for $\mathcal{I} = \{i_1, \dots, i_m\}$. As required, the size of the zero matrix is described by the subscript, i.e., $0_{n \times m} \in \mathbb{R}^{n \times m}$. Finally, a matrix M is said to be *Metzler*, if all the off-diagonal entries of M are nonnegative.

II. PRELIMINARIES

In this study, we deal with a large-scale bidirectional network whose general form is given as follows:

Definition 1: A linear system

$$\dot{x} = Ax + bu \quad (1)$$

with $A \in \mathbb{R}^{n \times n}$ and $b \in \mathbb{R}^n$ is said to be a *bidirectional network* (A, b) if A is stable and symmetric.

To simplify the arguments, we deal with only single-input systems, with similar results available also for multi-input

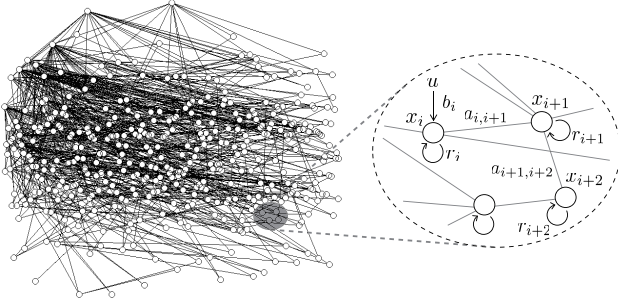


Fig. 1. Depiction of Bidirectional Networks.

cases [31], [33]. Typical examples of bidirectional networks include dynamical systems coupled by *undirected graphs* (see [4] for an overview of network systems and multi-agent systems). For example, let us examine the following spatially discrete reaction-diffusion system evolving over networks described by

$$\dot{x}_i = -r_i x_i + \sum_{j=1, j \neq i}^n a_{i,j} (x_j - x_i) + b_i u, \quad i \in \{1, \dots, n\} \quad (2)$$

where r_i denotes the reaction rate (chemical dissolution) of x_i , and $a_{i,j} = a_{j,i}$ for $i \neq j$ denotes the diffusion intensity between x_i and x_j (see Fig. 1). In this figure, each state x_i is assigned on a node, which is referred to as the i th node. The i th node has a self-loop, on which the reaction rate r_i is assigned. Furthermore, if $a_{i,j} \neq 0$, the i th and j th nodes are connected by an edge, on which the diffusion intensity $a_{i,j}$ is assigned. Throughout this paper, we use the same symbols of nodes, edges and self-loops as in Fig. 1 for depicting bidirectional networks.

System (2) is used as a primal model that represents diffusion processes evolving over complex networks (see Chapter 18 in [34]). The interconnection topology of this system can be represented in a graph-theoretic manner. By defining the reaction matrix $R := \text{diag}([r_1, \dots, r_n])$ and the symmetric weighted graph Laplacian $\mathcal{L} := \{l_{i,j}\}$ associated with

$$l_{i,j} = \begin{cases} -a_{i,j}, & i \neq j \\ \sum_{j=1, j \neq i}^n a_{i,j}, & i = j, \end{cases}$$

it is represented as one of the bidirectional networks with

$$A = -(R + \mathcal{L}), \quad b = \begin{bmatrix} b_1 \\ \vdots \\ b_n \end{bmatrix}$$

for the state vector $x := [x_1, \dots, x_n]^T$. Note that

$$\begin{bmatrix} r_1 \\ \vdots \\ r_n \end{bmatrix} = -A \mathbf{1}_n, \quad \mathbf{1}_n := \begin{bmatrix} 1 \\ \vdots \\ 1 \end{bmatrix} \in \mathbb{R}^n \quad (3)$$

follows from $\mathcal{L} \mathbf{1}_n = 0$. This coupled dynamics is stable if at least one r_i is strictly positive, $a_{i,j}$ are nonnegative for all i , and the graph is connected.

In this paper, we address two kinds of model reduction problems involving such bidirectional networks. To this end,

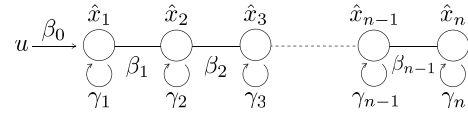


Fig. 2. Depiction of Positive Tridiagonal Realization.

we first introduce a state-space realization having a positive tridiagonal structure, which plays a central role in this study.

Definition 2: Let (A, b) be a bidirectional network. A unitary transformation by $H \in \mathbb{R}^{n \times n}$ is said to be *positive tridiagonalization*, if $\hat{A} := H^T A H \in \mathbb{R}^{n \times n}$ and $\hat{b} := H^T b \in \mathbb{R}_+^n$ are in the form of

$$\hat{A} = \begin{bmatrix} \alpha_1 & \beta_1 & & & & \\ \beta_1 & \alpha_2 & \beta_2 & & & \\ & \ddots & \ddots & \ddots & & \\ & & \ddots & \ddots & \beta_{n-1} & \\ & & & \beta_{n-1} & \alpha_n & \\ & & & & & \end{bmatrix}, \quad \hat{b} = \begin{bmatrix} \beta_0 \\ 0 \\ 0 \\ \vdots \\ 0 \end{bmatrix} \quad (4)$$

with $\beta_i \geq 0$ for all $i \in \{0, \dots, n-1\}$. Moreover, the pair (\hat{A}, \hat{b}) is referred to as a *positive tridiagonal realization*.

For the positive tridiagonal realization, the state vector is denoted by $\hat{x} = [\hat{x}_1, \dots, \hat{x}_n]^T := H^T x$. This realization has the following two properties. The first is *positivity*, i.e., it belongs to a class of positive systems because \hat{A} is Metzler and the entries of \hat{b} are all nonnegative (see [35], [36] for the general overview of positive systems). The second is a *tridiagonal structure*, i.e., it represents serially cascaded autonomous systems equipped with a boundary input (see Fig. 2). In this figure, γ_i and β_i denote the intensity of the reaction and the diffusion of \hat{x}_i , respectively, where each γ_i is given by

$$\begin{bmatrix} \gamma_1 \\ \vdots \\ \gamma_n \end{bmatrix} = -\hat{A} \mathbf{1}_n, \quad (5)$$

in a manner similar to (3). In the following sections, these properties of the positive tridiagonal realization will be fully exploited to analyze bidirectional networks. First, we show the existence and uniqueness of positive tridiagonalization as follows:

Theorem 1: For every bidirectional network (A, b) , there exists a transformation matrix $H \in \mathbb{R}^{n \times n}$ for positive tridiagonalization. Furthermore, for

$$i^* := \begin{cases} \min_{i \in \{1, \dots, n-1\}} \{i : \beta_i = 0\}, & \text{if } \prod_{i=1}^{n-1} \beta_i = 0 \\ n, & \text{otherwise,} \end{cases} \quad (6)$$

the submatrix $H e_{1:i^*}^n \in \mathbb{R}^{n \times i^*}$ is uniquely determined among all transformation matrices.

Effective tridiagonalization procedures for large matrices have been widely investigated in the control theory as well as the numerical linear algebra community for various applications such as eigenvalue computations and model reduction. For instance, the Householder transformation (Chapter 6 in [37]), the Lanczos procedure of Krylov projection methods (Chapter 10 in [5]), and the transformation into controller

Hessenberg form [38] for a symmetric matrix are well known. Although every symmetric matrix admits a tridiagonal form, the selection of the sign of each β_i is generally not considered in the literature such as [38]. On the other hand, this study focuses on the case in which all β_i are nonnegative, i.e., positive tridiagonal realization. The algorithm for positive tridiagonalization, which shows that the transformation always exists, is derived straightforwardly from the existing transformation such as the Householder transformation. See Appendix A for the proof.

In addition, the structure of (\hat{A}, \hat{b}) in (4) leads to i^* in (6) coinciding with the dimension of the controllable subspace of (A, b) . Thus the uniqueness of $He_{1:i^*}^n$ in Theorem 1 implies that the transformation matrix for positive tridiagonalization corresponding to the controllable subspace of (A, b) is uniquely determined. Appendix A contains this proof.

As for computational complexity, the above positive tridiagonalization procedure does not require computationally expensive operations. More specifically, if we adopt the primary algorithm based on the Householder transformation, its complexity is at most $(2/3)n^3$ even for dense matrices (see Chapter 6 in [37]). In addition, it is known that the complexity can be dramatically reduced to $\mathcal{O}(n)$ by explicitly taking advantage of particular matrix properties such as sparsity [5], [39]. In this sense, positive tridiagonalization can be implemented even for large-scale bidirectional networks.

Remark 1: Every (even nonsymmetric) tridiagonal matrix $\hat{A}' = \{\hat{a}'_{i,j}\}$ such that

$$\hat{a}'_{i,i+1}\hat{a}'_{i+1,i} \geq 0, \quad i \in \{1, \dots, n-1\}$$

is diagonally similar to a symmetric positive tridiagonal matrix \hat{A} , i.e., there exists a nonsingular diagonal matrix D such that $D\hat{A}'D^{-1} = \hat{A}$. Therefore, once the realization (\hat{A}', \hat{b}) is derived, it allows analyses similar to those in the following sections.

III. KRYLOV-BASED MODEL REDUCTION

The aim of this section is to provide a solution to the following problem of Krylov-based model reduction with a specified error precision. Hereafter, we denote the input-to-state transfer function of (A, b) by

$$g(s) := (sI_n - A)^{-1}b. \quad (7)$$

Problem 1: Consider a bidirectional network (A, b) , and define g in (7). Given a constant $\delta \geq 0$, find a k -dimensional approximant $\hat{g}^{(k)}$ such that $k \leq n$ and

$$\|g(s) - \hat{g}^{(k)}(s)\|_{\mathcal{H}_\infty} \leq \delta. \quad (8)$$

Our approach to solving Problem 1 is as follows. For a given bidirectional network (A, b) , we consider the k -dimensional projection based on positive tridiagonalization, i.e., the approximant is given by

$$\hat{g}^{(k)}(s) := H^{(k)}(sI_k - \hat{A}^{(k)})^{-1}\hat{b}^{(k)} \quad (9)$$

where

$$H^{(k)} := He_{1:k}^n, \quad \hat{A}^{(k)} := (H^{(k)})^\top AH^{(k)}, \quad \hat{b}^{(k)} := (H^{(k)})^\top b \quad (10)$$

Note that $\hat{A}^{(k)} \in \mathbb{R}^{k \times k}$ and $\hat{b}^{(k)} \in \mathbb{R}^k$ are given by truncating the positive tridiagonal realization (\hat{A}, \hat{b}) up to the k -dimension; in other words, they satisfy $\hat{A}^{(k)} = (e_{1:k}^n)^\top \hat{A} e_{1:k}^n$ and $\hat{b}^{(k)} = (e_{1:k}^n)^\top \hat{b}$. Then, the truncation error will be found to be characterized by its DC gain owing to the positivity of (\hat{A}, \hat{b}) ; moreover, it will be shown that the truncation error monotonically decreases as k increases by virtue of the tridiagonal structure of (\hat{A}, \hat{b}) . Thus, this error analysis will provide a solution to Problem 1, as shown in the following subsection.

A. Approximation Error Analysis based on Positive Tridiagonal Realization

First, we describe two fundamental lemmas valid for general single-input single-output positive systems. The first is well-known (see Theorem 4 in [40]).

Lemma 1: Consider a single-input single-output positive system $f(s) = c(sI_n - A)^{-1}b$, where $A \in \mathbb{R}^{n \times n}$ is Metzler and stable, $b \in \mathbb{R}_+^n$, and $c \in \mathbb{R}_+^{1 \times n}$. Then, $\|f(s)\|_{\mathcal{H}_\infty} = f(0)$.

This lemma shows that the \mathcal{H}_∞ -norm of every positive system is characterized by its DC gain. Using this lemma, we derive the second lemma, which will be used for truncation error analysis:

Lemma 2: Consider a single-input single-output positive system $f(s) = c(sI_n - A)^{-1}b$, where $A \in \mathbb{R}^{n \times n}$ is Metzler and stable, $b \in \mathbb{R}_+^n$, and $c \in \mathbb{R}_+^{1 \times n}$. Let $\mathcal{I} \subseteq \{1, \dots, n\}$ be given, and define the truncated model associated with \mathcal{I} by

$$f_{\mathcal{I}}(s) := c_{\mathcal{I}}(sI_{|\mathcal{I}|} - A_{\mathcal{I}})^{-1}b_{\mathcal{I}} \quad (11)$$

where $A_{\mathcal{I}} := (e_{\mathcal{I}}^n)^\top A e_{\mathcal{I}}^n \in \mathbb{R}^{|\mathcal{I}| \times |\mathcal{I}|}$, $b_{\mathcal{I}} := (e_{\mathcal{I}}^n)^\top b \in \mathbb{R}_+^{|\mathcal{I}|}$, and $c_{\mathcal{I}} := c e_{\mathcal{I}}^n \in \mathbb{R}_+^{1 \times |\mathcal{I}|}$. Then, for any \mathcal{I} , the truncated model $f_{\mathcal{I}}$ is stable and it satisfies

$$\|f(s) - f_{\mathcal{I}}(s)\|_{\mathcal{H}_\infty} = f(0) - f_{\mathcal{I}}(0). \quad (12)$$

Proof: Since any principal submatrix of stable Metzler matrices is also stable, $f_{\mathcal{I}}$ is stable (see Chapter 2.5 in [41]). In order to show the validity of (12), we first denote the error system by

$$f(s) - f_{\mathcal{I}}(s) = c_e(sI_{n+|\mathcal{I}|} - A_e)^{-1}b_e$$

where

$$A_e := \text{Diag}(A, A_{\mathcal{I}}), \quad b_e := \begin{bmatrix} b \\ -b_{\mathcal{I}} \end{bmatrix}, \quad c_e := \begin{bmatrix} c & c_{\mathcal{I}} \end{bmatrix}.$$

Note that $e_{\mathcal{I}}^n \in \mathbb{R}_+^{n \times |\mathcal{I}|}$ and $e_{\bar{\mathcal{I}}}^n \in \mathbb{R}_+^{n \times |\bar{\mathcal{I}}|}$ satisfy

$$e_{\mathcal{I}}^n (e_{\mathcal{I}}^n)^\top + e_{\bar{\mathcal{I}}}^n (e_{\bar{\mathcal{I}}}^n)^\top = I_n$$

with $\bar{\mathcal{I}} := \{1, \dots, n\} \setminus \mathcal{I}$. Then, the similarity transformation of the error system given by

$$V = \begin{bmatrix} (e_{\mathcal{I}}^n)^\top & I_{|\mathcal{I}|} \\ I_n & 0 \end{bmatrix}, \quad V^{-1} = \begin{bmatrix} 0 & I_n \\ I_{|\mathcal{I}|} & -(e_{\mathcal{I}}^n)^\top \end{bmatrix}$$

yields

$$VA_eV^{-1} = \begin{bmatrix} A_{\mathcal{I}} & (e_{\mathcal{I}}^n)^\top A e_{\mathcal{I}}^n (e_{\mathcal{I}}^n)^\top \\ 0 & A \end{bmatrix}, \quad Vb_e = \begin{bmatrix} 0 \\ b \end{bmatrix}, \\ c_eV^{-1} = \begin{bmatrix} c_{\mathcal{I}} & c e_{\bar{\mathcal{I}}}^n (e_{\bar{\mathcal{I}}}^n)^\top \end{bmatrix}$$

where the entries of Vb_e and c_eV^{-1} are all nonnegative, and VA_eV^{-1} is Metzler because $(e_{\mathcal{I}}^n)^T A e_{\mathcal{I}}^n \in \mathbb{R}_+^{|\mathcal{I}| \times |\mathcal{I}|}$ is composed of off-diagonal entries of A . Hence, applying Lemma 1 to this realization proves (12). ■

Lemma 2 shows that the maximal gain of not only positive systems, but also error systems is characterized by the DC gain. However, this lemma does not suggest how the system should be truncated. Thus, we further focus on the positive tridiagonal realization, which resolves this concern, as shown in the following theorem:

Theorem 2: Given a positive tridiagonal realization (\hat{A}, \hat{b}) , define

$$\hat{X}(s) := (sI_n - \hat{A})^{-1} \hat{b}, \quad \hat{X}^{(k)}(s) := (sI_k - \hat{A}^{(k)})^{-1} \hat{b}^{(k)} \quad (13)$$

where $\hat{A}^{(k)}$ and $\hat{b}^{(k)}$ are defined as in (10), and denote the i th entries of \hat{X} and $\hat{X}^{(k)}$ by \hat{X}_i and $\hat{X}_i^{(k)}$, respectively. Then, $\hat{X}_i^{(k)}$ is stable and it satisfies

$$\|\hat{X}_i(s) - \hat{X}_i^{(k)}(s)\|_{\mathcal{H}_\infty} = \hat{X}_i(0) - \hat{X}_i^{(k)}(0) \quad (14)$$

for all $i \in \{1, \dots, k\}$ and $k \in \{1, \dots, n\}$. In addition, the right-hand side of (14) monotonically decreases as k increases, and the truncation error, i.e., the value of the left-hand side of (14), is minimal among all k -dimensional truncated models of \hat{X}_i associated with any $\mathcal{I} \subseteq \{1, \dots, n\}$ satisfying $|\mathcal{I}| = k$.

Proof: The equality (14) follows from applying Lemma 2 to \hat{X}_i with $\mathcal{I} := \{1, \dots, k\}$ because \hat{X}_i is a single-input single-output positive system. In what follows, let us prove the monotonicity and minimality of the truncation error. To prove the monotonicity, it is sufficient to show that

$$\begin{aligned} & [\hat{X}_i(0) - \hat{X}_i^{(k)}(0)] - [\hat{X}_i(0) - \hat{X}_i^{(k+1)}(0)] \\ &= \hat{X}_i^{(k+1)}(0) - \hat{X}_i^{(k)}(0) \geq 0. \end{aligned}$$

Note that $\hat{X}_i^{(k)}$ is obtained by truncating the $(k+1)$ th state of $\hat{X}_i^{(k+1)}$. Hence, the inequality follows from applying Lemma 2 to $\hat{X}_i^{(k+1)}$ and its truncated model $\hat{X}_i^{(k)}$. Next, to prove the minimality, we consider $\tilde{\mathcal{I}}_\kappa$ such that $|\tilde{\mathcal{I}}_\kappa| = k$ and

$$\tilde{\mathcal{I}}_\kappa = \{1, \dots, \kappa\} \cup \mathcal{J}, \quad \mathcal{J} \subseteq \{\kappa+2, \dots, n\}$$

with $\kappa \in \{1, \dots, k\}$. Furthermore, we denote the truncated model of \hat{X}_i associated with $\tilde{\mathcal{I}}_\kappa$ by $\hat{X}_i^{\tilde{\mathcal{I}}_\kappa}$. Note that $\tilde{\mathcal{I}}_\kappa$ can represent all sets of indices such that $|\tilde{\mathcal{I}}_\kappa| = k$. First, we consider the case of $1 \in \tilde{\mathcal{I}}_\kappa$. Clearly, if $\kappa = k$, i.e., if $\mathcal{J} = \emptyset$, then $\hat{X}_i^{\tilde{\mathcal{I}}_\kappa} = \hat{X}_i^{(\kappa)}$ holds. If $\kappa < k$, we have

$$(e_{\tilde{\mathcal{I}}}^n)^T \hat{A} e_{\tilde{\mathcal{I}}}^n = \begin{bmatrix} \hat{A}^{(\kappa)} & 0 \\ 0 & (e_{\mathcal{J}}^n)^T \hat{A} e_{\mathcal{J}}^n \end{bmatrix}, \quad (e_{\tilde{\mathcal{I}}}^n)^T \hat{b} = \begin{bmatrix} \hat{b}^{(\kappa)} \\ 0 \end{bmatrix}$$

which follows from the structure of the tridiagonal realization. These imply that $\hat{X}_i^{\tilde{\mathcal{I}}_\kappa} = \hat{X}_i^{(\kappa)}$ holds for any \mathcal{J} and $i \in \{1, \dots, k\}$. Hence, it follows that

$$\begin{aligned} & \min_{\kappa \in \{1, \dots, k\}} \|\hat{X}_i(s) - \hat{X}_i^{\tilde{\mathcal{I}}_\kappa}(s)\|_{\mathcal{H}_\infty} \\ &= \min_{\kappa \in \{1, \dots, k\}} \|\hat{X}_i(s) - \hat{X}_i^{(\kappa)}(s)\|_{\mathcal{H}_\infty} \geq \|\hat{X}_i(s) - \hat{X}_i^{(k)}(s)\|_{\mathcal{H}_\infty} \end{aligned}$$

for all $i \in \{1, \dots, k\}$. Second, if $1 \notin \tilde{\mathcal{I}}_\kappa$, then $\hat{X}_i^{\tilde{\mathcal{I}}_\kappa} = 0$ follows from $(e_{\tilde{\mathcal{I}}_\kappa}^n)^T \hat{b} = 0$. Thus, for all $i \in \{1, \dots, k\}$, the error

$$\|\hat{X}_i(s) - \hat{X}_i^{\tilde{\mathcal{I}}_\kappa}(s)\|_{\mathcal{H}_\infty} = \hat{X}_i(0)$$

is larger than the right-hand side of (14). Hence, the minimality of the truncation error follows. ■

Theorem 2 states that we have the *exact* truncation error of the input-to-state mapping of the positive tridiagonal realization. Even though Lemma 2 shows that the maximum truncation error for every positive system can be evaluated by the DC gain, it is, in general, nontrivial to systematically determine a set \mathcal{I} that leads to better precision. On the other hand, Theorem 2 shows that retaining the first k states achieves the least truncation error, and that the resultant truncation error monotonically decreases as k increases due to the serially cascaded structure of the tridiagonal realization. The coordinate transformation of each $\hat{X}_i - \hat{X}_i^{(k)}$ in Theorem 2 back to the original one straightforwardly provides a solution to Problem 1 as follows:

Theorem 3: Given a bidirectional network (A, b) , let (\hat{A}, \hat{b}) be its positive tridiagonal realization, and $H \in \mathbb{R}^{n \times n}$ be its transformation matrix. Define g in (7) and

$$\begin{aligned} \Phi &:= H \text{diag}(-\hat{A}^{-1} \hat{b}) \in \mathbb{R}^{n \times n} \quad (15) \\ \hat{\Phi}^{(k)} &:= \begin{bmatrix} H^{(k)} \text{diag}(-\hat{A}^{(k)})^{-1} \hat{b}^{(k)} & 0_{n \times (n-k)} \end{bmatrix} \in \mathbb{R}^{n \times n} \end{aligned}$$

where $\hat{A}^{(k)}$, $\hat{b}^{(k)}$ and $H^{(k)}$ are defined as in (10). Then, $\hat{g}^{(k)}$ in (9) is stable and it satisfies

$$\|g(s) - \hat{g}^{(k)}(s)\|_{\mathcal{H}_\infty} \leq \sqrt{n} \|\Phi - \hat{\Phi}^{(k)}\|_{l_\infty}. \quad (16)$$

In addition, the right-hand side of (16) monotonically decreases as k increases.

Proof: We have

$$\begin{aligned} \|g(s) - \hat{g}^{(k)}(s)\|_{\mathcal{H}_\infty} &\leq \sqrt{\sum_{i=1}^n \|g_i(s) - \hat{g}_i^{(k)}(s)\|_{\mathcal{H}_\infty}^2} \\ &\leq \sqrt{n} \max_{i \in \{1, \dots, n\}} \|g_i(s) - \hat{g}_i^{(k)}(s)\|_{\mathcal{H}_\infty} \end{aligned}$$

where g_i and $\hat{g}_i^{(k)}$ denote the i th entries of g and $\hat{g}^{(k)}$, respectively. Note that $g = H\hat{X}$ and $\hat{g}^{(k)} = H^{(k)}\hat{X}^{(k)}$ hold, where \hat{X} and $\hat{X}^{(k)}$ are defined as in (13). Using Theorem 2, we have

$$\begin{aligned} \|g_i(s) - \hat{g}_i^{(k)}(s)\|_{\mathcal{H}_\infty} &= \left\| \sum_{j=1}^n h_{i,j} \{\hat{X}_j(s) - \hat{X}_j^{(k)}(s)\} \right\|_{\mathcal{H}_\infty} \quad (17) \\ &\leq \sum_{j=1}^n |h_{i,j}| \|\hat{X}_j(0) - \hat{X}_j^{(k)}(0)\| \\ &= \sum_{j=1}^n |h_{i,j}| \|\hat{X}_j(0) - \hat{X}_j^{(k)}(0)\| \\ &= \|\Phi_i - \hat{\Phi}_i^{(k)}\|_{l_\infty} \end{aligned}$$

where Φ_i and $\hat{\Phi}_i^{(k)}$ denote the i th row vectors of Φ and $\hat{\Phi}^{(k)}$, respectively, and $\hat{X}_j^{(k)}$ for each $j \in \{k+1, \dots, n\}$ is to be replaced with zero. Hence, (16) follows from

$$\max_{i \in \{1, \dots, n\}} \|\Phi_i - \hat{\Phi}_i^{(k)}\|_{l_\infty} = \|\Phi - \hat{\Phi}^{(k)}\|_{l_\infty}.$$

Finally, the monotonicity of the right-hand side of (16) follows from the monotonic decrease of $\hat{X}_j(0) - \hat{X}_j^{(k)}(0)$ in (17), which has been shown in Theorem 2. ■

Theorem 3 gives an \mathcal{H}_∞ -error bound of the approximant $\hat{g}^{(k)}$. Thus, the result directly works as the Krylov-based model reduction with a specified error precision. More precisely, finding the minimum k such that the right-hand side of (16) is less than $\delta \geq 0$, we obtain the k -dimensional approximant $\hat{g}^{(k)}$, which is a solution to Problem 1. Note that, since \hat{A} is tridiagonal and \hat{b} is a multiple of e_1^n , the vector $-\hat{A}^{-1}\hat{b}$ can be efficiently calculated as the solution x of the linear equation $\hat{A}x + \hat{b} = 0$. Actually, [42] proposed an algorithm to solve such tridiagonal equations with complexity $\log_2 n$.

It should be further noted that, independent of the sign of each β_i in (4), its k -dimensional truncated model yields the same transfer function, i.e., the *external* representation, $\hat{g}^{(k)}$, in (9). This means that the k th iteration of the Lanczos procedure of the Krylov projection methods indeed yields the same approximant. However, to the best of our knowledge, an a priori error bound like (16) has not yet been derived. The success of our approach results from introducing the transformation into the *positive* tridiagonal realization, i.e., an *internally positive* representation, by focusing on the symmetry of the system matrix A . This approximation with a specified error precision will also work effectively in Section IV.

Remark 2: Based on the above analysis, the Krylov-based model reduction of multi-output cases, i.e., (A, b) with $C \in \mathbb{R}^{p \times n}$, is also attained by

$$\|Cg(s) - C\hat{g}^{(k)}(s)\|_{\mathcal{H}_\infty} \leq \sqrt{p} \|C(\Phi - \hat{\Phi}^{(k)})\|_{l_\infty},$$

which is proven in a manner similar to the proof of Theorem 3.

B. Large-Scale Example: Krylov-based Model Reduction of a Complex Network System

In this subsection, we show the efficiency of Theorem 3 through an example of the model reduction of a large-scale bidirectional network. Let us consider a diffusion process evolving over the Holme-Kim model [1] composed of 3000 nodes and 6000 edges, whose interconnection topology is depicted in Fig. 3. In this figure, we use the same symbols of nodes and edges as those in Fig. 1 to show the interconnection topology. This network is an extension of the Barabasi-Albert model, which is one of the best-known complex network models. Actually, the Holme-Kim model is known to have a scale-free and small-world property as well as a high cluster coefficient.

The bidirectional network (A, b) considered here is fixed as follows. The input affects only one node, i.e., $b = e_1^{3000}$. For $A \in \mathbb{R}^{3000 \times 3000}$ in (2), we randomly choose the diffusion terms $a_{i,j}$ from $(0, 1]$ if nodes i and j for $i \neq j$ are connected, otherwise they are set to 0, and we give the reaction terms as $r_1 = 1$ and $r_i = 0$ for all $i \in \{2, \dots, 3000\}$.

The positive tridiagonalization of (A, b) yields (\hat{A}, \hat{b}) with its transformation matrix H , for which Fig. 4 depicts the value of the reaction term γ_k in (5) (the broken line) and the value of the diffusion term β_k in (4) (the line of *) versus each k in the horizontal axis. In this figure, since no remarkable

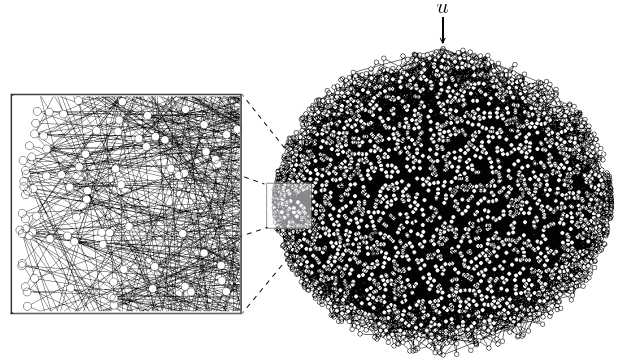


Fig. 3. Holme-Kim Model with 3000 Nodes and 6000 Edges.

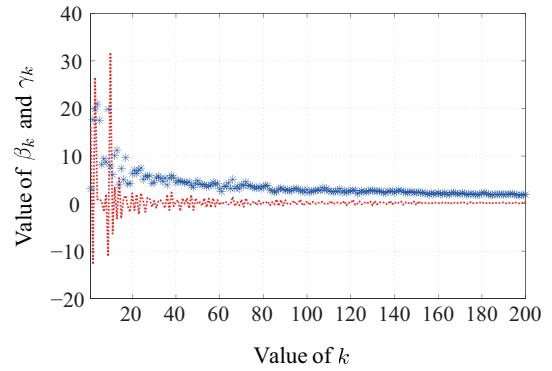


Fig. 4. Plots of Diffusion Term β_k (Line of *) and Reaction Term γ_k (Broken Line) of \hat{A} .

changes appear after $k = 200$, we show the plots of only the first 200 values. We can see that the reaction of \hat{x}_k and the diffusion between \hat{x}_k and \hat{x}_{k+1} become weaker as k increases. This tendency suggests that \hat{x}_k for $k \gg 1$ makes a smaller contribution to the input-to-state mapping.

Furthermore, Fig. 5 shows the right-hand side of (16) in the logarithmic scale for each value of k . It is found that the error bound rapidly decreases as k increases. When we give the admissible error bound $\delta = 1.0 \times 10^{-4}$ in (8), the minimum k such that the right-hand side of (16) is less than δ is 110. This implies that the input-to-state mapping of the 3000-dimensional system g in (7) is well approximated by the 110-dimensional approximant $\hat{g}^{(k)}$ in (9).

This numerical experiment is implemented in MATLAB 2007b on a computer equipped with Intel Core i7 CPU-M620, 2.67 GHz, RAM 6.00 GB, and a 64-bit operating system. As for the computation time, it takes 20.6 [sec] to find Φ in (15), which includes the implementation of the positive tridiagonalization, and 0.25 [sec] to calculate the right-hand side of (16) for $k = 110$.

IV. CLUSTERING-BASED STATE AGGREGATION

In Section III, we established a systematic Krylov-based model reduction procedure for bidirectional networks based on positive tridiagonalization. Without relying on computationally expensive operations, the procedure yields an approximant of the transfer function that conforms to a specified error precision. However, the procedure necessarily imposes the

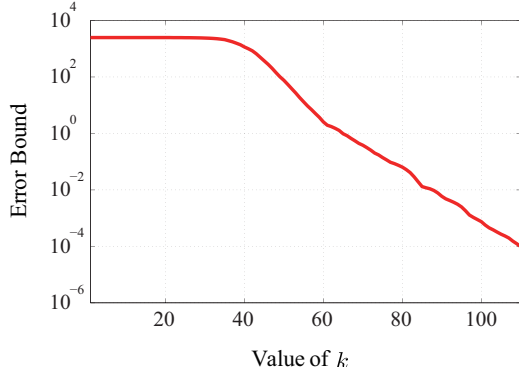


Fig. 5. Plots of Error Bound.

tridiagonal structure on the state-space realization of the approximant independent of the original system. This means that the reduced model does not preserve any interconnection topology of the original bidirectional network. Actually, the same difficulty is confronted by most traditional model reduction methods, such as the balanced truncation, the Hankel-norm approximation, and the Krylov projection methods [5], [6]. To overcome this difficulty, we provide in this section a novel model reduction method that is implemented through state aggregation. The main feature of this method is to preserve network topology among node sets, called clusters, and also guarantee a specified error precision. In addition, it is found that the Krylov-based model reduction proposed in Section III is an efficient tool for evaluating the resultant aggregation error.

A. Problem Formulation

In this subsection, we formulate a network topology-preserving model reduction problem. To this end, we begin with the following definition of state aggregation:

Definition 3: Let (A, b) be a bidirectional network. The family of an index set $\{\mathcal{I}_{[l]}\}_{l \in \mathbb{L}}$ for $\mathbb{L} := \{1, \dots, L\}$ is called a *cluster set*, each of whose elements is referred to as a cluster if each element $\mathcal{I}_{[l]}$ is a disjoint subset of $\{1, \dots, n\}$ such that

$$\bigcup_{l \in \mathbb{L}} \mathcal{I}_{[l]} = \{1, \dots, n\}. \quad (18)$$

Furthermore, an *aggregation matrix* compatible with $\{\mathcal{I}_{[l]}\}_{l \in \mathbb{L}}$ is defined by

$$P := \text{Diag}(p_{[1]}, \dots, p_{[L]})\Pi \in \mathbb{R}^{L \times n} \quad (19)$$

with $p_{[l]} \in \mathbb{R}^{1 \times |\mathcal{I}_{[l]}|}$ such that $\|p_{[l]}\| = 1$, and the permutation matrix

$$\Pi := \begin{bmatrix} (e_{\mathcal{I}_{[1]}}^n)^T \\ \vdots \\ (e_{\mathcal{I}_{[L]}}^n)^T \end{bmatrix} \in \mathbb{R}^{n \times n}, \quad e_{\mathcal{I}_{[l]}}^n \in \mathbb{R}^{n \times |\mathcal{I}_{[l]}|}. \quad (20)$$

Then, the *aggregated model* of (A, b) associated with P is denoted by (PAP^T, Pb) , and its transfer function is defined by

$$\hat{g}(s) := P^T(sI_L - PAP^T)^{-1}Pb. \quad (21)$$

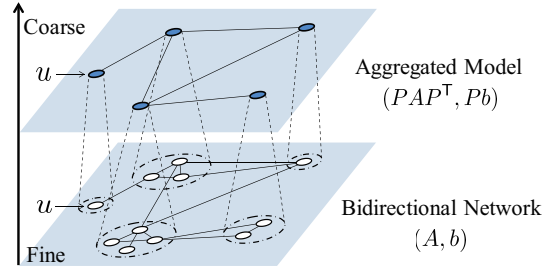


Fig. 6. Illustration of Clustering-based State Aggregation.

In this definition, PAP^T is symmetric, and the aggregation matrix P clearly satisfies $PP^T = I_L$. In the rest of this section, we denote the index with respect to each cluster $\mathcal{I}_{[l]}$ by the subscript of $[l]$. For this clustering-based state aggregation, we give the following intuitive explanation. There are L clusters labeled by $l \in \mathbb{L}$. Each node of the original network belongs to exactly one of the clusters, or, in other words, the state variable of the l th cluster is represented by

$$x_{[l]} := (e_{\mathcal{I}_{[l]}}^n)^T x \in \mathbb{R}^{|\mathcal{I}_{[l]}|},$$

where $\mathcal{I}_{[l]}$ satisfies $\mathcal{I}_{[l]} \cap \mathcal{I}_{[l']} = \emptyset$ for $l \neq l'$ and (18). Under this definition, the linear transformation $\hat{x} = Px$ by the aggregation matrix (19) implies that

$$\hat{x}_{[l]} = p_{[l]}x_{[l]}, \quad l \in \mathbb{L},$$

where $\hat{x}_{[l]} \in \mathbb{R}$ is a scalar. This transformation implies that the original state $x_{[l]} \in \mathbb{R}^{|\mathcal{I}_{[l]}|}$ is aggregated into $\hat{x}_{[l]} \in \mathbb{R}$ by weighting $p_{[l]} \in \mathbb{R}^{1 \times |\mathcal{I}_{[l]}|}$. Then the clustering-based state aggregation problem considered herein is formulated as follows:

Problem 2: Consider a bidirectional network (A, b) , and define g in (7). Given a constant $\epsilon \geq 0$, find a cluster set $\{\mathcal{I}_{[l]}\}_{l \in \mathbb{L}}$ and an aggregation matrix P in (19) compatible with $\{\mathcal{I}_{[l]}\}_{l \in \mathbb{L}}$ such that

$$\|g(s) - \hat{g}(s)\|_{\mathcal{H}_\infty} \leq \epsilon, \quad (22)$$

where \hat{g} is defined as in (21).

In traditional model reduction methods, each state of the reduced model is usually obtained as a linear combination of *all* states of the original system; in other words, the projection matrix has no specific structure. This clearly contrasts with our problem formulation, where the aggregation matrix (19) is *block-diagonally structured*. Consequently, as shown in Fig. 6, where each cluster of the original bidirectional network is depicted by the circle of the chain-line, the interconnection topology (spatial distribution) among clusters is retained through reduction.

Our approach to solving Problem 2 is as follows. First, in Section IV-B, we define an *exactly reducible cluster* for the state aggregation. This is done based on a notion of cluster uncontrollability, which implies that the states of nodes in a cluster have the same trajectory for any input signal under the same initial condition. Then, we will show that the cluster reducibility is characterized by linear dependence of row vectors of Φ that is introduced in (15); in other words, it

follows that the cluster reducibility of $\mathcal{I}_{[l]}$ is equivalent to the rank deficiency of $(e_{\mathcal{I}_{[l]}}^n)^\top \Phi$. Next, in Section IV-C, we relax the exact notion of cluster reducibility to a weak notion, which is defined as *near* rank deficiency of $(e_{\mathcal{I}_{[l]}}^n)^\top \Phi$. Then, it will be shown that the distance to the rank deficiency of $(e_{\mathcal{I}_{[l]}}^n)^\top \Phi$ has a linear relation to the approximation error that is caused by the aggregation of weakly reducible clusters. Finally, based on this error analysis, a specific construction algorithm of the aggregation matrix, i.e., an algorithm to determine a cluster set $\{\mathcal{I}_{[l]}\}_{l \in \mathbb{L}}$ and the corresponding aggregation weights $p_{[l]}$, will be provided in Section IV-D.

B. Exact Cluster Reducibility

First, let us consider how *reducibility of a cluster* should be formulated for the aggregation. For example, consider the cluster of $\mathcal{I}_{[1]} = \{1, 2, 3\}$. If the state variables x_i for $i \in \mathcal{I}_{[1]}$ in this cluster have the same behavior, namely

$$x_1(t) = x_2(t) = x_3(t)$$

holds for all $t \geq 0$, under any input signal and $x(0) = 0$, they should be aggregated for reduction. This case, in fact, means that only its one-dimensional subspace

$$\{(x_1, x_2, x_3) : x_1 = x_2 = x_3\}$$

is controllable. In other words, the transfer functions from u to $x_1 - x_2$ and $x_2 - x_3$ are inevitably zero, or equivalently the transfer function of the cluster $\mathcal{I}_{[1]}$ should be in the form of

$$(e_{\mathcal{I}_{[1]}}^n)^\top g(s) = \begin{bmatrix} 1 \\ 1 \\ 1 \end{bmatrix} \bar{g}_{[1]}(s)$$

for a scalar rational function $\bar{g}_{[1]}$. This observation is generalized as follows:

Definition 4: Consider a bidirectional network (A, b) , and define g in (7). Under the notation in Definition 3, a cluster $\mathcal{I}_{[l]}$ is said to be *reducible* if there exist a scalar rational function $\bar{g}_{[l]}$ and a vector $\eta_{[l]} \in \mathbb{R}^{|\mathcal{I}_{[l]}|}$ such that

$$(e_{\mathcal{I}_{[l]}}^n)^\top g(s) = \eta_{[l]} \bar{g}_{[l]}(s). \quad (23)$$

In order to characterize (23) in an algebraic manner, we use the matrix $\Phi \in \mathbb{R}^{n \times n}$ that is introduced in Theorem 3:

Theorem 4: Given a bidirectional network (A, b) , let (\hat{A}, \hat{b}) be its positive tridiagonal realization and, $H \in \mathbb{R}^{n \times n}$ be its transformation matrix. Define Φ in (15). Then, a cluster $\mathcal{I}_{[l]}$ is reducible if and only if there exist a row vector $\bar{\phi}_{[l]} \in \mathbb{R}^{1 \times n}$ and a vector $\eta_{[l]} \in \mathbb{R}^{|\mathcal{I}_{[l]}|}$ such that

$$(e_{\mathcal{I}_{[l]}}^n)^\top \Phi = \eta_{[l]} \bar{\phi}_{[l]}. \quad (24)$$

In addition, if (24) holds, then $\eta_{[l]}$ is a multiple of

$$-(e_{\mathcal{I}_{[l]}}^n)^\top A^{-1}b.$$

Moreover, if all clusters $\mathcal{I}_{[l]}$ are reducible, then the aggregated model (PAP^\top, Pb) in Definition 3 with $p_{[l]} = \eta_{[l]}^\top / \|\eta_{[l]}\|$ is stable and it satisfies

$$g(s) = \hat{g}(s), \quad (25)$$

where \hat{g} is defined as in (21).

Proof: [Proof of (23) \Leftrightarrow (24)] Suppose that (23) holds. Consider i^* in (6) representing the dimension of the controllable sub-space of (\hat{A}, \hat{b}) , and define

$$\mathcal{J} := \{1, \dots, i^*\}, \quad \bar{\mathcal{J}} := \{i^* + 1, \dots, n\}.$$

Since $\hat{X}_k(s) \equiv 0$ holds for $k \in \bar{\mathcal{J}}$, where \hat{X}_k is the k th entry of \hat{X} in (13), we have

$$\hat{X}(s) = e_{\mathcal{J}}^n (e_{\mathcal{J}}^n)^\top \hat{X}(s). \quad (26)$$

In addition, note that

$$g(s) = H(sI_n - \hat{A})^{-1} \hat{b} = H \hat{X}(s)$$

holds by definition. Then, from this fact and (26), we see that (23) is equivalent to

$$(e_{\mathcal{I}_{[l]}}^n)^\top H e_{\mathcal{J}}^n (e_{\mathcal{J}}^n)^\top \hat{X}(s) = \eta_{[l]} \bar{g}_{[l]}(s). \quad (27)$$

It should be emphasized that the functions \hat{X}_k for $k \in \mathcal{J}$ are *linearly independent* because any two of them do not have the same relative degree, i.e., the difference of degrees between the denominator and the numerator polynomials, due to the serially cascaded structure of the positive tridiagonal realization. This fact implies that there exists a row vector $\bar{h}_{[l]} \in \mathbb{R}^{1 \times i^*}$ such that

$$(e_{\mathcal{I}_{[l]}}^n)^\top H e_{\mathcal{J}}^n = \eta_{[l]} \bar{h}_{[l]}, \quad (28)$$

which means that the rank of $(e_{\mathcal{I}_{[l]}}^n)^\top H e_{\mathcal{J}}^n \in \mathbb{R}^{|\mathcal{I}_{[l]}| \times i^*}$ is one. Note that

$$\text{diag}(-\hat{A}^{-1} \hat{b}) = e_{\mathcal{J}}^n (e_{\mathcal{J}}^n)^\top \text{diag}(-\hat{A}^{-1} \hat{b})$$

follows from (26) and $\hat{X}(0) = -\hat{A}^{-1} \hat{b}$. Multiplying (28) by $(e_{\mathcal{J}}^n)^\top \text{diag}(-\hat{A}^{-1} \hat{b})$ from the right side, we have

$$(e_{\mathcal{I}_{[l]}}^n)^\top H e_{\mathcal{J}}^n (e_{\mathcal{J}}^n)^\top \text{diag}(-\hat{A}^{-1} \hat{b}) = \eta_{[l]} \bar{h}_{[l]} (e_{\mathcal{J}}^n)^\top \text{diag}(-\hat{A}^{-1} \hat{b})$$

where the left-hand side is equal to $(e_{\mathcal{I}_{[l]}}^n)^\top \Phi$. This implies that

$$\bar{\phi}_{[l]} := \bar{h}_{[l]} (e_{\mathcal{J}}^n)^\top \text{diag}(-\hat{A}^{-1} \hat{b}) \in \mathbb{R}^{1 \times n}$$

satisfies (24). Hence, (23) \Rightarrow (24) is proven. For the proof of (24) \Rightarrow (23), see the proof of Theorem 5 because this is a special case of Theorem 5. In addition, substituting $s = 0$ to (23), which is equivalent to (24), proves that $\eta_{[l]}$ is a multiple of $-(e_{\mathcal{I}_{[l]}}^n)^\top A^{-1}b$.

[Proof of (25)] Consider a matrix $q_{[l]} \in \mathbb{R}^{(|\mathcal{I}_{[l]}|-1) \times |\mathcal{I}_{[l]}|}$ such that $[p_{[l]}^\top, q_{[l]}^\top]^\top \in \mathbb{R}^{|\mathcal{I}_{[l]}| \times |\mathcal{I}_{[l]}|}$ is unitary, and define

$$Q := \text{Diag}(q_{[1]}, \dots, q_{[L]}) \Pi \in \mathbb{R}^{(n-L) \times n}, \quad (29)$$

which is an orthogonal complement of P in (19). Here, we allow empty $q_{[l]}$ if $|\mathcal{I}_{[l]}| = 1$. Considering the similarity transformation for the error system $g - \hat{g}$, we have

$$\begin{aligned} V A_e V^{-1} &= \begin{bmatrix} P A P^\top & P A Q^\top Q \\ 0 & A \end{bmatrix}, & V b_e &= \begin{bmatrix} 0 \\ b \end{bmatrix}, \\ c_e V^{-1} &= [P^\top \quad Q^\top Q] \end{aligned} \quad (30)$$

where

$$A_e := \text{Diag}(A, PAP^T), \quad b_e := \begin{bmatrix} b \\ -Pb \end{bmatrix}, \quad c_e := [I_n \quad P^T].$$

and

$$V = \begin{bmatrix} P & I_L \\ I_n & 0 \end{bmatrix}, \quad V^{-1} = \begin{bmatrix} 0 & I_n \\ I_L & -P \end{bmatrix}.$$

The block structure of (30) implies that the error system is in the cascaded form of

$$g(s) - \hat{g}(s) = \Xi(s)Q^T Qg(s) \quad (31)$$

where

$$\Xi(s) := P^T(sI_L - PAP^T)^{-1}PA + I_n.$$

The reducibility of all clusters and $p_{[l]} = \eta_{[l]}^T / \|\eta_{[l]}\|$ imply that $Qg = 0$. Hence, (25) follows. ■

Theorem 4 implies that the cluster reducibility (23) is characterized by linear dependence among the row vectors of Φ . More specifically, the distance between the i th and j th row vectors of Φ represents the closeness between the behavior of x_i and x_j . Furthermore, from the fact that $\eta_{[l]}$ must be a multiple of $-(e_{\mathcal{I}_{[l]}}^n)^T A^{-1}b$ if $\mathcal{I}_{[l]}$ is reducible, we see that, to achieve the exact state aggregation (25), we are required to take the aggregation weights $p_{[l]}$ that are compatible with the DC gain $g(0) = -A^{-1}b$ and a cluster set $\{\mathcal{I}_{[l]}\}_{l \in \mathcal{L}}$ satisfying the reducibility. However, (23) or, equivalently, (24) is restrictive in general. This is because it represents a kind of local uncontrollability such that the controllable subspace of $x_{[l]} = (e_{\mathcal{I}_{[l]}}^n)^T x$ is one-dimensional.

Example: To demonstrate Theorem 4, let us consider a simple bidirectional network (A, b) given by

$$A = \begin{bmatrix} -7 & 1 & 1 & 2 & 2 \\ 1 & -1 & & & \\ 1 & & -1 & & \\ 2 & & & -2 & \\ 2 & & & & -2 \end{bmatrix}, \quad b = \begin{bmatrix} 1 \\ 0 \\ 0 \\ 0 \\ 0 \end{bmatrix}$$

whose interconnection topology is depicted in the left side of Fig. 7. In this figure, we use the same symbols as those in Fig. 1. The symmetric topology with respect to permutation suggests that the trajectories of x_2 and x_3 , as well as those of x_4 and x_5 are identical if $x_2(0) = x_3(0)$ and $x_4(0) = x_5(0)$. This is equivalent to saying that $g_2 = g_3$ and $g_4 = g_5$, where g_i denotes the i th entry of the transfer function g in (7). In terms of Definition 4, for the clusters

$$\mathcal{I}_{[1]} = \{1\}, \quad \mathcal{I}_{[2]} = \{2, 3\}, \quad \mathcal{I}_{[3]} = \{4, 5\},$$

which are depicted by the circles of the chain line in the left side of Fig. 7, there exists a scalar function $\bar{g}_{[l]}$ for each $l \in \{1, 2, 3\}$ such that (23) holds, where both $\eta_{[2]}$ and $\eta_{[3]}$ must be a multiple of $[1, 1]^T$.

On the other hand, by the positive tridiagonalization of (A, b) , we obtain (\hat{A}, \hat{b}) with its transformation matrix $H \in \mathbb{R}^{5 \times 5}$ as

$$\hat{A} = \left[\begin{array}{ccc|cc} -7.00 & 3.16 & & & \\ 3.16 & -1.80 & 0.40 & & \\ & 0.40 & -1.20 & 0 & \\ \hline & & & -1.50 & 0.50 \\ & & & 0.50 & -1.50 \end{array} \right], \quad \hat{b} = \begin{bmatrix} 1 \\ 0 \\ 0 \\ 0 \\ 0 \end{bmatrix}$$

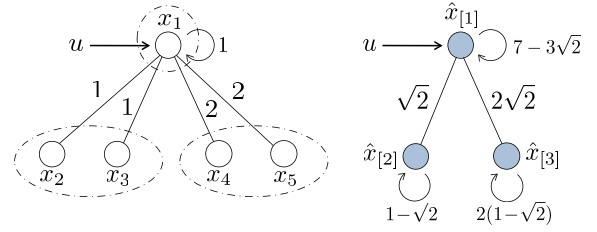


Fig. 7. Depiction of Interconnected Topologies.

and

$$H = \left[\begin{array}{ccc|cc} 1 & 0 & 0 & 0 & 0 \\ 0 & 0.316 & 0.63 & -0.50 & -0.50 \\ 0 & 0.316 & 0.63 & -0.50 & -0.50 \\ 0 & 0.63 & -0.32 & 0.50 & -0.50 \\ 0 & 0.63 & -0.32 & 0.50 & -0.50 \end{array} \right].$$

Note that the third off-diagonal entry of \hat{A} is zero. This implies that the dimension of the controllable subspace of (\hat{A}, \hat{b}) is $i^* = 3$ in (6). In addition, the submatrix $H e_{1:3}^5 \in \mathbb{R}^{5 \times 3}$, i.e., the first three column vectors of H , is uniquely determined as shown in Theorem 1. Using these matrices, we construct the index matrix Φ in (15) as

$$\Phi = H \text{diag}(-\hat{A}^{-1}\hat{b}) = \begin{bmatrix} 1 & 0 & 0 & 0 & 0 \\ 0 & 0.60 & 0.40 & 0 & 0 \\ 0 & 0.60 & 0.40 & 0 & 0 \\ 0 & 1.20 & -0.20 & 0 & 0 \\ 0 & 1.20 & -0.20 & 0 & 0 \end{bmatrix}$$

where the second and third row vectors, and the fourth and fifth row vectors are identical, respectively. This implies that there exists a row vector $\bar{\phi}_{[l]} \in \mathbb{R}^{1 \times 5}$ for each $l \in \{1, 2, 3\}$ such that (24) holds, where both $\eta_{[2]}$ and $\eta_{[3]}$ must be a multiple of $[1, 1]^T$. Since the DC gain of (A, b) is $-A^{-1}b = [1, \dots, 1]^T$, each $\eta_{[l]}$ coincides with a multiple of $-(e_{\mathcal{I}_{[l]}}^n)^T A^{-1}b$ as shown in Theorem 4.

For this cluster set $\{\mathcal{I}_{[l]}\}_{l \in \{1, 2, 3\}}$ and the corresponding aggregation weights $p_{[l]} = \eta_{[l]}^T / \|\eta_{[l]}\|$, we have the aggregation matrix in (19) as

$$P = \begin{bmatrix} 1 & 0 & 0 & 0 & 0 \\ 0 & 1/\sqrt{2} & 1/\sqrt{2} & 0 & 0 \\ 0 & 0 & 0 & 1/\sqrt{2} & 1/\sqrt{2} \end{bmatrix}.$$

Consequently, we obtain the aggregated model

$$PAP^T = \begin{bmatrix} -7 & \sqrt{2} & 2\sqrt{2} \\ \sqrt{2} & -1 & 0 \\ 2\sqrt{2} & 0 & -2 \end{bmatrix}, \quad Pb = \begin{bmatrix} 1 \\ 0 \\ 0 \end{bmatrix},$$

which satisfies $g = \hat{g}$. The interconnection topology of this aggregated model is depicted in the right side of Fig. 7.

Remark 3: The exact state aggregation in Theorem 4 coincides with the elimination of a kind of locally uncontrollable subspace of (A, b) . It should be emphasized that this aggregation is different from the standard elimination of the uncontrollable subspace in the sense that the aggregation matrix P in (19) is block-diagonally structured.

C. Cluster Reducibility Relaxation

In what follows, aiming at significant order reduction, we relax (23) through its equivalent representation of (24).

Definition 5: Given a bidirectional network (A, b) , let (\hat{A}, \hat{b}) be its positive tridiagonal realization, and $H \in \mathbb{R}^{n \times n}$ be its transformation matrix. Define Φ in (15), and let $\eta_{[l]} \in \mathbb{R}^{|\mathcal{I}_{[l]}|}$ be a vector. A cluster $\mathcal{I}_{[l]}$ is said to be θ -reducible with respect to $\eta_{[l]}$ if there exists a row vector $\bar{\phi}_{[l]} \in \mathbb{R}^{1 \times n}$ such that

$$\left\| (e_{\mathcal{I}_{[l]}}^n)^T \Phi - \eta_{[l]} \bar{\phi}_{[l]} \right\|_{l_\infty} \leq \theta, \quad \theta \geq 0. \quad (32)$$

In Definition 5, the constant θ represents the degree of cluster reducibility. The vector $\eta_{[l]}$ determines the aggregation weight for a cluster $\mathcal{I}_{[l]}$. Note that $\eta_{[l]}$ can be chosen arbitrary as long as (32) is satisfied. This degree of freedom can be used to give some additional property to the aggregated model (see Section IV-D for details). Next, we show that the approximation error caused by the state aggregation is easily evaluated when all clusters are θ -reducible. To this end, we first give the following lemma:

Lemma 3: Given a bidirectional network (A, b) , let (\hat{A}, \hat{b}) be its positive tridiagonal realization, and $H \in \mathbb{R}^{n \times n}$ be its transformation matrix. Define Φ in (15). Then

$$\|Cg(s)\|_{\mathcal{H}_\infty} \leq \sqrt{\bar{p}} \|C\Phi\|_{l_\infty}$$

holds for any output mapping $C \in \mathbb{R}^{p \times n}$.

We can prove this lemma in a manner similar to Theorem 3. Now we are in a position to present the main theorem of this section.

Theorem 5: Given a bidirectional network (A, b) , let (\hat{A}, \hat{b}) be its positive tridiagonal realization, and $H \in \mathbb{R}^{n \times n}$ be its transformation matrix. Consider the state aggregation with P in Definition 3. If all clusters $\mathcal{I}_{[l]}$ are θ -reducible with respect to each $\eta_{[l]}$, then the aggregated model (PAP^T, Pb) in Definition 3 with $p_{[l]} = \eta_{[l]}^T / \|\eta_{[l]}\|$ is stable and it satisfies

$$\|g(s) - \hat{g}(s)\|_{\mathcal{H}_\infty} \leq \sqrt{\alpha} \|(PAP^T)^{-1}PA\| \theta, \quad (33)$$

where \hat{g} is defined as in (21) and $\alpha := \sum_{l=1}^L |\mathcal{I}_{[l]}| (|\mathcal{I}_{[l]}| - 1)$.

Proof: The stability of \hat{g} follows from the negative definiteness of A . Under the notation in the proof of Theorem 4

$$\|g(s) - \hat{g}(s)\|_{\mathcal{H}_\infty} \leq \|\Xi(s)\|_{\mathcal{H}_\infty} \|Q^T Qg(s)\|_{\mathcal{H}_\infty} \quad (34)$$

follows from (31). First, let us prove that

$$\|\Xi(s)\|_{\mathcal{H}_\infty} = \|(PAP^T)^{-1}PA\|.$$

The inequality $\|\Xi\|_{\mathcal{H}_\infty} < \gamma$ holds if and only if $\gamma > \|I_n\| = 1$ and the Hamiltonian $\gamma^2(\gamma^2 - 1)^{-1}J(\gamma)$ of Ξ where

$$J(\gamma) := \begin{bmatrix} PAP^T & -\gamma^{-1}PAA^T P^T \\ \gamma^{-1}I_L & -PA^T P^T \end{bmatrix}$$

has no eigenvalue on the imaginary axis (see Proposition 5.4 in [5]). Note that this J is identical to the Hamiltonian of

$$\hat{\Xi}(s) := (sI_L - PAP^T)^{-1}PA. \quad (35)$$

Thus, $\|\Xi\|_{\mathcal{H}_\infty} < \gamma$ is equivalent to $\gamma > 1$ and $\|\hat{\Xi}\|_{\mathcal{H}_\infty} < \gamma$. On the other hand, by $I_n = P^T P + Q^T Q$ and $PP^T = I_L$, we obtain

$$\begin{aligned} \|\hat{\Xi}(0)\| &= \|(PAP^T)^{-1}PA(P^T P + Q^T Q)\| \\ &= \|P + Z\| = \lambda_{\max}^{\frac{1}{2}}(I_L + ZZ^T) > 1, \end{aligned}$$

where $PZ^T = 0$ holds for $Z := (PAP^T)^{-1}PAQ^T Q$. Hence, $\|\Xi\|_{\mathcal{H}_\infty} < \gamma$ holds if and only if $\|\hat{\Xi}\|_{\mathcal{H}_\infty} < \gamma$ holds for all $\gamma \geq 0$. Thus, we have $\|\Xi\|_{\mathcal{H}_\infty} = \|\hat{\Xi}\|_{\mathcal{H}_\infty}$. Finally, applying Lemma 4 in Appendix B to $\hat{\Xi}$ proves

$$\|\Xi(s)\|_{\mathcal{H}_\infty} = \|\hat{\Xi}(0)\| = \|(PAP^T)^{-1}PA\|. \quad (36)$$

Next, we evaluate $\|Q^T Qg\|_{\mathcal{H}_\infty}$. From

$$\begin{aligned} \|Q^T Qg(s)\|_{\mathcal{H}_\infty} &= \sup_{\omega \in \mathbb{R}} \lambda_{\max}^{\frac{1}{2}}(g^T(-j\omega)Q^T Qg(j\omega)) \\ &= \|Qg(s)\|_{\mathcal{H}_\infty}, \end{aligned}$$

where the second equality comes from $QQ^T = I_{n-L}$, it follows that

$$\begin{aligned} \|Q^T Qg(s)\|_{\mathcal{H}_\infty} &= \left\| \begin{bmatrix} q_{[1]}(e_{\mathcal{I}_{[1]}}^n)^T g(s) \\ \vdots \\ q_{[L]}(e_{\mathcal{I}_{[L]}}^n)^T g(s) \end{bmatrix} \right\|_{\mathcal{H}_\infty} \\ &\leq \sqrt{\sum_{l=1}^L \|q_{[l]}(e_{\mathcal{I}_{[l]}}^n)^T g(s)\|_{\mathcal{H}_\infty}^2}. \end{aligned}$$

Using Lemma 3 with $C = q_{[l]}(e_{\mathcal{I}_{[l]}}^n)^T \in \mathbb{R}^{(|\mathcal{I}_{[l]}|-1) \times n}$, we have

$$\|q_{[l]}(e_{\mathcal{I}_{[l]}}^n)^T g(s)\|_{\mathcal{H}_\infty} \leq \sqrt{|\mathcal{I}_{[l]}| - 1} \|q_{[l]}(e_{\mathcal{I}_{[l]}}^n)^T \Phi\|_{l_\infty}.$$

By the assumption of θ -reducibility, it is also obtained that $\|\Delta_{[l]}\|_{l_\infty} \leq \theta$, where $\Delta_{[l]} := (e_{\mathcal{I}_{[l]}}^n)^T \Phi - \eta_{[l]} \bar{\phi}_{[l]}$. From the fact that $[p_{[l]}^T, q_{[l]}^T]^T$ is unitary and $p_{[l]} = \eta_{[l]}^T / \|\eta_{[l]}\|$, it follows that $q_{[l]}(e_{\mathcal{I}_{[l]}}^n)^T \Phi = q_{[l]} \Delta_{[l]}$. Hence, we have

$$\begin{aligned} \|q_{[l]}(e_{\mathcal{I}_{[l]}}^n)^T \Phi\|_{l_\infty} &\leq \|q_{[l]}\|_{l_\infty} \|\Delta_{[l]}\|_{l_\infty} \\ &\leq \sqrt{|\mathcal{I}_{[l]}|} \|q_{[l]}\| \theta \leq \sqrt{|\mathcal{I}_{[l]}|} \theta \end{aligned}$$

where the second inequality comes from $\|M\|_{l_\infty} \leq \sqrt{m} \|M\|$ for any $M \in \mathbb{R}^{n \times m}$ and the third from $\|q_{[l]}\| = 1$. Finally, we have

$$\|Q^T Qg(s)\|_{\mathcal{H}_\infty} \leq \sqrt{\sum_{l=1}^L |\mathcal{I}_{[l]}| (|\mathcal{I}_{[l]}| - 1)} \theta \quad (37)$$

that proves the claim. \blacksquare

Theorem 5 shows a linear relation between the aggregation error $\|g - \hat{g}\|_{\mathcal{H}_\infty}$ and the parameter θ that represents the degree of cluster reducibility. Thus, we can use θ as a design criterion to assign the coarseness of the resultant aggregated model. However, the error evaluation based on (33), especially in a large-scale setting, may become conservative. Therefore, using the Krylov-based model reduction in Section III, we will provide a more practical error evaluation in the following subsection, even though (33) gives a reasonable cluster determination strategy.

Remark 4: The error bound in (33) is not a priori computable because it depends on P . On the other hand, admitting more conservative evaluation, we can derive an a priori error

bound. More specifically, we can verify that α is bounded by $n(n-1)$ and $\|(PAP^T)^{-1}PA\|$ is bounded by

$$\|(PAP^T)^{-1}PA\| \leq -\frac{\lambda_{\max}(A) + \lambda_{\min}(A)}{2\sqrt{\lambda_{\max}(A)\lambda_{\min}(A)}}. \quad (38)$$

The inequality (38) is proven as follows. For $\hat{\Xi}$ in (35) and a given $\gamma > 0$, $\|(PAP^T)^{-1}PA\| = \|\hat{\Xi}\|_{\mathcal{H}_\infty} < \gamma$ holds if there exists a positive definite matrix $X \in \mathbb{R}^{L \times L}$ such that

$$XPAP^T + PA^T P^T X + \gamma^{-1}(XPAA^T P^T X + I_L) \quad (39)$$

is negative definite. This condition can be derived based on the standard bounded real lemma. We suppose that the explicit solution is $X = aI_L$, where $a > 0$ will be determined later. Note that (39) with $X = aI_L$ is equal to

$$P\{2aA + \gamma^{-1}(a^2A^2 + I_n)\}P^T.$$

From eigenvalue decomposition, it follows that $2aA + \gamma^{-1}(a^2A^2 + I_n)$ is negative definite if

$$f(a\lambda(A)) < \gamma, \quad f(x) := \frac{x + x^{-1}}{2}$$

holds for all eigenvalues $\lambda(A)$ of A . Since $f(x)$ is convex for $x \in (-\infty, 0)$, the maximum of $f(a\lambda(A))$ is attained at either $a\lambda_{\min}(A)$ or $a\lambda_{\max}(A)$. Thus, $\|\hat{\Xi}\|_{\mathcal{H}_\infty} < \gamma$ follows for

$$\gamma > \max\{f(a\lambda_{\min}(A)), f(a\lambda_{\max}(A))\}.$$

From the fact that the minimum of the right-hand side is attained by $a = (\lambda_{\max}(A)\lambda_{\min}(A))^{-1/2}$, the inequality (38) follows. It should be noted that $\lambda_{\min}(A)$ and $\lambda_{\max}(A)$ can be efficiently calculated by using existing methods, e.g., the power method (see Chapter 10 in [5]).

D. Clustering-based State Aggregation Procedure

In this subsection, based on the error analysis in Section IV-C, we present a procedure of clustering-based state aggregation. This subsection is divided into the following three parts. In Section IV-D1), we show three methods for determining $\eta_{[l]}$ in Definition 5, to give some additional property to the aggregated model. In Section IV-D2), we propose a greedy algorithm to construct a cluster set $\{\mathcal{I}_{[l]}\}_{l \in \mathbb{L}}$ satisfying θ -reducibility, which does not depend on the specific choice of $\eta_{[l]}$. In Section IV-D3), we derive a tighter error bound, which is efficient especially for large-scale systems. Finally, we establish a procedure of clustering-based state aggregation.

1) *A Priori Form of Aggregation Weights*: Recall that, according to Theorem 5, the aggregation weights are given by $p_{[l]} = \eta_{[l]}^T / \|\eta_{[l]}\|$. Without loss of generality, we can write $\eta_{[l]}$ as

$$\eta_{[l]} = (e_{\mathcal{I}_{[l]}}^n)^T \eta \quad (40)$$

using a vector $\eta \in \mathbb{R}^n$. Here, we propose three methods for a priori determination of η to give some additional property to the aggregated model. The first one is $\eta = -A^{-1}b$. This η is reasonable in the sense that (32) is equivalent to (24) if $\theta = 0$. This is proven by the fact that, as shown in Theorem 4, $\eta_{[l]}$ necessarily coincides with a multiple of $-(e_{\mathcal{I}_{[l]}}^n)^T A^{-1}b$ if a cluster $\mathcal{I}_{[l]}$ is exactly reducible. In addition, the aggregation weight

Input: $\theta \geq 0$, $\eta \in \mathbb{R}^n$, and $\Phi \in \mathbb{R}^{n \times n}$
Output: A set $\{\mathcal{I}_{[l]}\}_{l \in \mathbb{L}}$ of θ -reducible clusters
1: $\mathbb{L} \leftarrow \{\}, \{\mathcal{I}_{[l]}\}_{l \in \mathbb{L}} \leftarrow \{\}$
2: **while** $\{\mathcal{I}_{[l]}\}_{l \in \mathbb{L}} \neq \{1, \dots, n\}$ **do**
3: Choose $j \in \{1, \dots, n\} \setminus \{\mathcal{I}_{[l]}\}_{l \in \mathbb{L}}$
4: $\mathbb{L} \leftarrow \{\mathbb{L}, |\mathbb{L}| + 1\}$, $\mathcal{I}_{[|\mathbb{L}|]} \leftarrow \{j\}$
5: **for** $i \in \{1, \dots, n\} \setminus \{\mathcal{I}_{[l]}\}_{l \in \mathbb{L}}$ **do**
6: **if** i and j satisfy (41) **then**
7: $\mathcal{I}_{[|\mathbb{L}|]} \leftarrow \{\mathcal{I}_{[|\mathbb{L}|]}, i\}$
8: **end if**
9: **end for**
10: **end while**

Fig. 8. Algorithm to Construct Set of θ -reducible Clusters.

$p_{[l]}$ assigned by this η is sufficient to guarantee the exact preservation of the steady-state characteristic, i.e., $g(0) = \hat{g}(0)$ holds for any $\{\mathcal{I}_{[l]}\}_{l \in \mathbb{L}}$. This is proven by $Qg(0) = 0$ in (31).

Furthermore, admitting possibly more conservative order reduction, we may obtain some properties by choosing η different from $-A^{-1}b$ as follows.

- $\eta = [1, \dots, 1]^T$: each state of the aggregated model represents the averaged state of the original bidirectional network.
- η such that $A\eta = \lambda_{\max}(A)\eta$: the dominant decay rate is preserved, i.e., it follows that $\lambda_{\max}(A) = \lambda_{\max}(PAP^T)$.

2) *Construction of Cluster Set*: We propose a greedy algorithm to construct a cluster set $\{\mathcal{I}_{[l]}\}_{l \in \mathbb{L}}$ satisfying θ -reducibility, on the premise that $\theta \geq 0$ and $\eta \in \mathbb{R}^n$ are given and Φ in (15) is obtained. Assume that a set of clusters $\{\mathcal{I}_{[1]}, \dots, \mathcal{I}_{[l]}\}$ are already made and let

$$\mathcal{J} := \{1, \dots, n\} \setminus \{\mathcal{I}_{[1]}, \dots, \mathcal{I}_{[l]}\}.$$

When we make a new cluster $\mathcal{I}_{[l+1]}$, we first choose an index $j \in \mathcal{J}$, and then look for indices $i \in \mathcal{J}$ satisfying

$$\|\phi_i - \eta_i \eta_j^{-1} \phi_j\|_{l_\infty} \leq \theta \quad (41)$$

where $\phi_i \in \mathbb{R}^{1 \times n}$ denotes the i th row vector of Φ and $\eta_i \in \mathbb{R}$ denotes the i th entry of η . Since (41) corresponds to taking $\bar{\phi}_{[l]} = \eta_j^{-1} \phi_j$ for (32), it is straightforward to verify that this newly constructed cluster is θ -reducible. This choice of $\bar{\phi}_{[l]}$ is reasonable because, in (41), the scale of $\eta_i \eta_j^{-1} \phi_j$ is adjusted to ϕ_i accordingly to the aggregation weight, even though there are the other choices of $\bar{\phi}_{[l]}$ to attain θ -reducibility. Figure 8 shows an algorithm for creating clusters based on (41), which requires at most $n(n-1)/2$ multiplications (vector norm calculations).

3) *Error Evaluation for Large-Scale Setting*: The conservativeness of the error bound in Theorem 5 depends on the estimation accuracy of $\|Q^T Qg\|_{\mathcal{H}_\infty} = \|Qg\|_{\mathcal{H}_\infty}$ in (37). Here, because of no explicit use of the information on Q , (37) may give a conservative error bound, especially for large-scale systems. In this sense, Theorem 5 does not necessarily give a satisfactory error bound, even though it gives us a reasonable cluster determination strategy. To compensate for this weakness, we use (33) along with a tighter error bound

shown in the following theorem. In this theorem, we utilize the Krylov-based model reduction in Section III to efficiently estimate $\|Qg\|_{\mathcal{H}_\infty}$ within a small error precision δ .

Theorem 6: Under the notation in Theorems 3 and 5, if k satisfies

$$\sqrt{n} \|\Phi - \hat{\Phi}^{(k)}\|_{l_\infty} \leq \delta, \quad (42)$$

then the aggregated model (PAP^T, Pb) associated with P satisfies

$$\|g(s) - \hat{g}(s)\|_{\mathcal{H}_\infty} \leq \|(PAP^T)^{-1}PA\|(\|Q\hat{g}^{(k)}(s)\|_{\mathcal{H}_\infty} + \delta), \quad (43)$$

where $\hat{g}^{(k)}$ is defined as in (9) and Q is an orthogonal complement of P such that $[P^T, Q^T]^T$ is unitary.

Proof: From (34) and (36), we have

$$\|g(s) - \hat{g}(s)\|_{\mathcal{H}_\infty} \leq \|(PAP^T)^{-1}PA\| \|Qg(s)\|_{\mathcal{H}_\infty}.$$

If (42) holds, then $\|g - \hat{g}^{(k)}\|_{\mathcal{H}_\infty} \leq \delta$ follows from Theorem 3. Hence, from $\|Q\| = 1$ and

$$\begin{aligned} \|Qg(s)\|_{\mathcal{H}_\infty} &\leq \|Q\hat{g}^{(k)}(s)\|_{\mathcal{H}_\infty} + \|Q\| \|g(s) - \hat{g}^{(k)}(s)\|_{\mathcal{H}_\infty} \\ &\leq \|Q\hat{g}^{(k)}(s)\|_{\mathcal{H}_\infty} + \delta, \end{aligned} \quad (44)$$

(43) follows. \blacksquare

Theorem 6 provides an alternative error bound, practically tight as long as $\delta \geq 0$ is sufficiently small. It should be remarked that once a desirable approximant $\hat{g}^{(k)}$ is obtained, the error bound (43) can be calculated efficiently because it consists only of the lower-dimensional components, i.e., $(PAP^T)^{-1}PA \in \mathbb{R}^{L \times n}$ and the k -dimensional system $Q\hat{g}^{(k)}$. Moreover, Q in (29) can be easily constructed.

To take advantage of error bounds in (33) and (43), we use both of them simultaneously, that is, we use

$$F(\theta) := \min\{\sqrt{\alpha} \|(PAP^T)^{-1}PA\|\theta, \|(PAP^T)^{-1}PA\|(\|Q\hat{g}^{(k)}(s)\|_{\mathcal{H}_\infty} + \delta)\}, \quad (45)$$

i.e., the minimum of the right-hand sides of (33) and (43). This combined error bound is more reasonable because the latter one provides tighter evaluation for middle and large θ . This is simply confirmed by the fact the latter is bounded owing to $\|Q\| = 1$ for any θ .

Based on the above arguments, a solution to Problem 2 with a given admissible error ϵ is provided by the following procedure:

Procedure of Clustering-based State Aggregation:

- (a) Prescribe a nonnegative constant δ .
- (b) Calculate the positive tridiagonal realization (\hat{A}, \hat{b}) in (4) with its transformation matrix H .
- (c) Find the minimum k satisfying (42), and then construct an approximant $\hat{g}^{(k)}$ in (9).
- (d) Set a vector $\eta \in \mathbb{R}^n$ in (40).
- (e) For a fixed θ , construct a cluster set $\{\mathcal{I}_{[l]}\}_{l \in \mathbb{L}}$ satisfying θ -reducibility by applying the algorithm in Fig. 8, and define the corresponding aggregation weights $p_{[l]} = \eta_{[l]}^T / \|\eta_{[l]}\|$, which determine P and Q in (19) and (29), respectively.
- (f) If $F(\theta)$ in (45) is not less than ϵ , then return to (e) by setting a smaller θ .

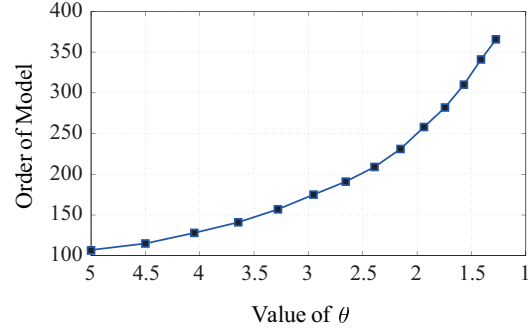


Fig. 9. Order of Resulting Models versus Values of θ .

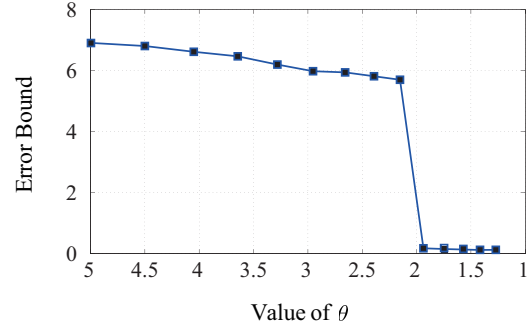


Fig. 10. Error Bound versus Values of θ .

The major computational effort is summarized as follows: (b) the positive tridiagonalization requires the complexity of $\mathcal{O}(n)$ or at most $(2/3)n^3$ [37], [39]; (c) the construction of Φ in (15), which coincides with solving linear equations for tridiagonal systems, requires the complexity of $\log_2 n$ [42]; and (e) the construction of a cluster set requires at most $n(n-1)/2$ multiplications. Finally, even though the explicit computational complexity of (f) is not available because matrix and system norms are usually calculated by convergence processes, it can be effectively implemented owing to the computational load reduction based on Theorem 6.

Remark 5: The value of δ in the above procedure corresponds to the estimation accuracy of $\|Qg\|_{\mathcal{H}_\infty}$, as shown in (44). Generally speaking, δ should be much smaller than a given ϵ so that the error bound (43) makes sense. However, setting an extremely small δ possibly loses the advantage of computational load reduction. In a practical sense, it is sufficient that δ is less than ϵ by several orders of magnitude.

E. Large-Scale Example: Clustering-based State Aggregation of a Complex Network System

We applied the proposed clustering-based state aggregation to the 3000-dimensional system dealt with in Section III-B, to solve Problem 2 with $\epsilon = 0.27$. This corresponds to an approximately 0.5% relative error because $\|g\|_{\mathcal{H}_\infty} = \|g(0)\| = 54.8$, where the first equation follows from Lemma 4 in Appendix B.

Let us implement the procedures (a)–(f) proposed in Section IV-D. Note that we obtained $k = 110$ -dimensional approximant $\hat{g}^{(k)}$, whose error is bounded by $\delta = 1.0 \times 10^{-4}$, in Section III-B. This means that the procedures (a)–(c) have

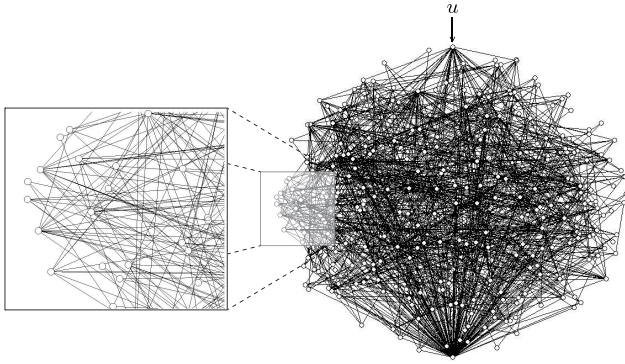


Fig. 11. Clustered Topology of the Holme-Kim Model (276 Clusters).

already been terminated. Thus, what remains to be implemented are the procedures (e)–(f). We perform (e)–(f) with the initial value of $\theta = 5.0$, and then iterate them with smaller values of θ . Against each value of θ , Figs. 9 and 10 depict the resultant order of aggregated models, i.e., the resultant number of clusters, and the resultant error bound, i.e., the value of $F(\theta)$ in (45), respectively. These figures show that the order of the aggregated model gradually increases, and the error bound appropriately decreases as θ decreases. Therefore, this result confirms that θ successfully captures the coarseness of the aggregated models to be constructed.

When $\theta = 1.82$, we obtain a 276-dimensional aggregated model shown in Fig. 11, where we use the same symbols of nodes (aggregated clusters) and edges as those in Fig. 1, and we omit the self-loops for simplicity. Its approximation error is bounded by 0.16, which is less than the prescribed $\epsilon = 0.27$. Comparing Fig. 11 with Fig. 3, we see that the interconnection topology of the aggregated model is much simpler than the original one. This example shows that the proposed method successfully extracts meaningful inter-cluster connections in the sense of input-to-state mapping approximations.

This numerical experiment is performed under the same setup in Section III-B. As for the computation time of one implementation of (e)–(f), it takes 23 [sec] to find an aggregation matrix P , which includes the construction of the cluster set $\{\mathcal{I}_{[l]}\}_{l \in \mathbb{L}}$, and 427 [sec] to evaluate its aggregation error. Finally, for comparison, the exact error $\|g - \hat{g}\|_{\mathcal{H}_\infty}$ is directly calculated. It takes 38927 [sec] for the calculation, and the resultant value is 0.070. Therefore, this result shows that the computational load reduction based on Theorem 6 is effective.

V. CONCLUSION

In this paper, two kinds of model reduction methods for large-scale bidirectional networks are proposed. Both methods fully exploit a network structure transformation implemented as positive tridiagonalization. First, we proposed a Krylov-based model reduction method with an \mathcal{H}_∞ -error bound, where the system, not necessarily positive, is transformed into a positive system with a tridiagonal structure. The positivity property is used in conjunction with the tridiagonal structure to derive an error bound for input-to-state model reduction. Next, we proposed a network clustering-based model reduction method, where the connection topology among clusters,

i.e., disjoint sets of nodes, is preserved. By introducing the reducibility of cluster sets, which coincides with local uncontrollability of the state-space, the method aggregates the states of each reducible cluster into lower-dimensional ones. The cluster reducibility can be efficiently characterized by means of positive tridiagonalization, and the state discrepancy between the original system and the reduced-order model is evaluated in terms of the \mathcal{H}_∞ -norm. The efficiency of both methods is verified through some numerical examples including application to a large-scale complex network system.

It should be emphasized that since positive tridiagonalization does not require computationally expensive operations, the proposed methods are applicable to even large-scale complex network systems. Obviously, all of the results stated in this paper involve a dual notion by considering the state-to-output mapping. Extension to directed networks is currently under investigation.

APPENDIX A EXISTENCE AND UNIQUENESS OF POSITIVE TRIDIAGONALIZATION

The existence of positive tridiagonalization can be easily proven through Householder transformation [37]. For reference, we show an algorithm for the positive tridiagonalization. For arbitrary $x \in \mathbb{R}^n$ and $y \in \mathbb{R}^n$ such that $\|x\| = \|y\|$ and $x \neq y$, define the symmetric unitary matrix

$$H = I_n - \frac{2(x - y)(x - y)^\top}{\|x - y\|^2} \in \mathbb{R}^{n \times n},$$

then the product of H , which is known as the Householder transformation, satisfies $y = Hx$. In what follows, we prove the existence of positive tridiagonalization of every bidirectional network (A, b) by induction. First, there exists the Householder transformation $b_1 = H_0 b$ such that $b_1 = \|b\| e_1^n$. Since $H_0 \in \mathbb{R}^{n \times n}$ is symmetric and unitary, the similarity transformation $A_1 := H_0 A H_0 \in \mathbb{R}^{n \times n}$ preserves the symmetry. Next, let us assume that a symmetric matrix $A_k \in \mathbb{R}^{n \times n}$ and a vector $b_k \in \mathbb{R}^n$ are in the form of

$$A_k = \left[\begin{array}{c|c} \hat{A}^{(k)} & 0_{(k-1) \times (n-k)} \\ \hline 0_{(n-k) \times (k-1)} & x \end{array} \right], \quad b_k = \begin{bmatrix} \beta_0 \\ 0 \\ \vdots \\ 0 \end{bmatrix}$$

where $\beta_0 \geq 0$, $x \in \mathbb{R}^{n-k}$, and $\hat{A}^{(k)} \in \mathbb{R}^{k \times k}$ being a symmetric tridiagonal matrix with nonnegative off-diagonal entries. Considering the Householder transformation $\tilde{x} = \tilde{H}_k x$ such that $\tilde{x} := \|x\| e_1^{n-k}$, we have

$$\begin{aligned} A_{k+1} &:= H_k A_k H_k \\ &= \left[\begin{array}{c|c} \hat{A}^{(k)} & 0_{(k-1) \times (n-k)} \\ \hline 0_{(n-k) \times (k-1)} & \tilde{x} \end{array} \right] \end{aligned}$$

and $b_{k+1} := H_k b_k = b_k$ where $H_k := \text{Diag}(I_k, \tilde{H}_k)$. Note that the $(k+1)$ -dimensional principal submatrix of A_{k+1} is a tridiagonal matrix having nonnegative off-diagonal entries. Thus, repeating this argument ensures the existence of the

transformation matrix $H := H_0 H_1 \cdots H_n$ for the positive tridiagonalization.

Next, we prove the uniqueness stated in Theorem 1. Suppose that both (\hat{A}, \hat{b}) and $(T\hat{A}T^T, T\hat{b})$ are positive tridiagonal realizations for a unitary matrix T . To prove the uniqueness, it is sufficient to show that T necessarily has the form of $T = \text{Diag}(I_{\bar{i}}, *)$. The fact that $T\hat{b}$ is a multiple of e_1^n and T is unitary leads to

$$T = \begin{bmatrix} 1 & 0 & 0 \\ 0 & t_{11} & t_{1*} \\ 0 & t_{*1} & \bar{T} \end{bmatrix} \quad (46)$$

where $t_{11} \in \mathbb{R}$, $t_{1*}^T, t_{*1} \in \mathbb{R}^{n-2}$ and $\bar{T} \in \mathbb{R}^{(n-2) \times (n-2)}$. Partitioning \hat{A} according to (46), we have

$$\hat{A} = \begin{bmatrix} \alpha_1 & \beta_1 & 0 \\ \beta_1 & \alpha_2 & \bar{\beta}^T \\ 0 & \bar{\beta} & \bar{A} \end{bmatrix}, \quad T\hat{A}T^T = \begin{bmatrix} \alpha_1 & \beta_1 t_{11} & \beta_1 t_{*1}^T \\ t_{11} \beta_1 & \bar{\alpha} & * \\ t_{*1} \beta_1 & * & * \end{bmatrix}$$

where $\bar{A} \in \mathbb{R}^{(n-2) \times (n-2)}$, $\bar{\beta} \in \mathbb{R}^{n-2}$ and

$$\bar{\alpha} = t_{11}^2 \alpha_2 + t_{1*} \bar{\beta} t_{11} + t_{11} \bar{\beta}^T t_{1*}^T + t_{1*} \bar{A} t_{1*}^T.$$

Since $T\hat{A}T^T$ is tridiagonal and $\beta_1 \neq 0$, we have $t_{*1} = 0$. In addition

$$TT^T = \begin{bmatrix} 1 & 0 & 0 \\ 0 & t_{11}^2 + t_{1*} t_{1*}^T & t_{1*} \bar{T}^T \\ 0 & \bar{T} t_{1*}^T & \bar{T} \bar{T}^T \end{bmatrix}$$

is I_n and \bar{T} is nonsingular. Thus, $t_{1*} = 0$ and $t_{11}^2 = 1$. Moreover, $t_{11} = 1$ follows from $t_{11} \beta_1 > 0$. Repeating this argument for $\beta_i \neq 0$ completes the proof.

APPENDIX B

Lemma 4: Any stable $A = A^T \in \mathbb{R}^{n \times n}$ and $B \in \mathbb{R}^{n \times m}$ satisfy $\|(sI_n - A)^{-1}B\|_{\mathcal{H}_\infty} = \|A^{-1}B\|$.

Proof: Denote $f(s) := (sI_n - A)^{-1}B$. By definition, $\|f(s)\|_{\mathcal{H}_\infty} \geq \|f(0)\|$ holds. To prove $\|f(s)\|_{\mathcal{H}_\infty} \leq \|f(0)\|$, let γ be an arbitrary number larger than $\|f(0)\|$. It suffices to show $\|f(s)\|_{\mathcal{H}_\infty} < \gamma$ or, equivalently,

$$J(\gamma) := \begin{bmatrix} A & -\gamma^{-1}BB^T \\ \gamma^{-1}I_n & -A^T \end{bmatrix}$$

has no eigenvalue on the imaginary axis. By the symmetry of A , we have

$$J^2(\gamma) = \begin{bmatrix} A^2 - \gamma^{-2}BB^T & * \\ 0 & A^2 - \gamma^{-2}BB^T \end{bmatrix}.$$

Note that the block-diagonal entry $A(I_n - \gamma^{-2}f(0)f^T(0))A^T$ is symmetric and positive definite owing to $\gamma > \|f(0)\|$. Therefore, all eigenvalues of J^2 are positive real. This directly indicates that all eigenvalues of J are nonzero real. This completes the proof. ■

ACKNOWLEDGMENT

This research is supported by the Aihara Innovative Mathematical Modelling Project, the Japan Society for the Promotion of Science (JSPS) through the ‘‘Funding Program for World-Leading Innovative R&D on Science and Technology (FIRST Program),’’ initiated by the Council for Science and Technology Policy (CSTP).

REFERENCES

- [1] S. Boccaletti, V. Latora, Y. Moreno, M. Chavez, and D.-U. Hwang, ‘‘Complex networks: Structure and dynamics,’’ *Physics reports*, vol. 424, no. 4, pp. 175–308, 2006.
- [2] S. H. Strogatz, ‘‘Exploring complex networks,’’ *Nature*, vol. 410, no. 6825, pp. 268–276, 2001.
- [3] Y.-Y. Liu, J.-J. Slotine, and A.-L. Barabási, ‘‘Controllability of complex networks,’’ *Nature*, vol. 473, no. 7346, pp. 167–173, 2011.
- [4] M. Mesbahi and M. Egerstedt, *Graph theoretic methods in multiagent networks*. Princeton University Press, 2010.
- [5] A. C. Antoulas, *Approximation of large-scale dynamical systems*. Society for Industrial and Applied Mathematics, 2009, vol. 6.
- [6] —, ‘‘An overview of model reduction methods and a new result,’’ in *Decision and Control, held jointly with the 28th Chinese Control Conference (CDC/CCC), 2009 Proceedings of the 48th IEEE Conference on*. IEEE, 2009, pp. 5357–5361.
- [7] W. H. Schilders, H. A. Van der Vorst, and J. Rommes, *Model order reduction: theory, research aspects and applications*. Springer, 2008, vol. 13.
- [8] D. F. Enns, ‘‘Model reduction with balanced realizations: An error bound and a frequency weighted generalization,’’ in *Decision and Control (CDC), 1984 Proceedings of the 23rd IEEE Conference on*, vol. 23. IEEE, 1984, pp. 127–132.
- [9] D. G. Meyer, ‘‘Fractional balanced reduction: Model reduction via fractional representation,’’ *Automatic Control, IEEE Transactions on*, vol. 35, no. 12, pp. 1341–1345, 1990.
- [10] K. Glover, ‘‘All optimal Hankel-norm approximations of linear multi-variable systems and their L_∞ -error bounds,’’ *International Journal of Control*, vol. 39, no. 6, pp. 1115–1193, 1984.
- [11] W.-Y. Yan and J. Lam, ‘‘An approximate approach to H_2 optimal model reduction,’’ *Automatic Control, IEEE Transactions on*, vol. 44, no. 7, pp. 1341–1358, 1999.
- [12] H. Sandberg and R. M. Murray, ‘‘Model reduction of interconnected linear systems,’’ *Optimal Control Applications and Methods*, vol. 30, no. 3, pp. 225–245, 2009.
- [13] Y. V. Genin and S. Kung, ‘‘A two-variable approach to the model reduction problem with Hankel norm criterion,’’ *Circuits and Systems, IEEE Transactions on*, vol. 28, no. 9, pp. 912–924, 1981.
- [14] K. Gallivan, A. Vandendorpe, and P. Van Dooren, ‘‘Model reduction via truncation: an interpolation point of view,’’ *Linear algebra and its applications*, vol. 375, pp. 115–134, 2003.
- [15] A. Astolfi, ‘‘Model reduction by moment matching for linear and nonlinear systems,’’ *Automatic Control, IEEE Transactions on*, vol. 55, no. 10, pp. 2321–2336, 2010.
- [16] K. Gallivan, A. Vandendorpe, and P. Van Dooren, ‘‘Model reduction of MIMO systems via tangential interpolation,’’ *SIAM Journal on Matrix Analysis and Applications*, vol. 26, no. 2, pp. 328–349, 2004.
- [17] A. C. Antoulas, C. A. Beattie, and S. Gugercin, *Interpolatory model reduction of large-scale dynamical systems*. Springer, 2010.
- [18] S. Gugercin, ‘‘Projection methods for model reduction of large-scale dynamical systems,’’ Ph.D. dissertation, Rice University, 2002.
- [19] S. Gugercin and K. Willcox, ‘‘Krylov projection framework for Fourier model reduction,’’ *Automatica*, vol. 44, no. 1, pp. 209–215, 2008.
- [20] S. Gugercin, A. C. Antoulas, and C. Beattie, ‘‘ H_2 model reduction for large-scale linear dynamical systems,’’ *SIAM journal on matrix analysis and applications*, vol. 30, no. 2, pp. 609–638, 2008.
- [21] H. Sandberg, ‘‘Hankel-norm-based lumping of interconnected linear systems,’’ in *Proceedings of MATHMOD 2009, Vienna, Austria*, 2009.
- [22] S. Lall, P. Krysyl, and J. E. Marsden, ‘‘Structure-preserving model reduction for mechanical systems,’’ *Physica D: Nonlinear Phenomena*, vol. 184, no. 1, pp. 304–318, 2003.
- [23] R.-C. Li and Z. Bai, ‘‘Structure-preserving model reduction,’’ in *Applied Parallel Computing. State of the Art in Scientific Computing*. Springer, 2006, pp. 323–332.
- [24] C. A. Beattie and S. Gugercin, ‘‘Interpolation theory for structure-preserving model reduction,’’ in *Decision and Control (CDC), 2008 Proceedings of the 47th IEEE Conference on*. IEEE, 2008, pp. 4204–4208.
- [25] J. Chow and P. Kokotovic, ‘‘Time scale modeling of sparse dynamic networks,’’ *Automatic Control, IEEE Transactions on*, vol. 30, no. 8, pp. 714–722, 1985.
- [26] E. Bryik and M. Arcak, ‘‘Area aggregation and time-scale modeling for sparse nonlinear networks,’’ *Systems & Control Letters*, vol. 57, no. 2, pp. 142–149, 2008.

- [27] J. Kurabayashi and K. Tsumura, "Approximation of large-scaled dynamical systems based on multi-layered hierarchical structure and multiple time scales," in *ICCAS-SICE, 2009*. IEEE, 2009, pp. 1058–1062.
- [28] P. Twu, M. Egerstedt, and S. Martini, "Controllability of homogeneous single-leader networks," in *Decision and Control (CDC), 2010 Proceedings of the 49th IEEE Conference on*. IEEE, 2010, pp. 5869–5874.
- [29] A. Chapman and M. Mesbahi, "UAV flocking with wind gusts: Adaptive topology and model reduction," in *American Control Conference (ACC), 2011*. IEEE, 2011, pp. 1045–1050.
- [30] T. Ishizaki, K. Kashima, and J. Imura, "Extraction of 1-dimensional reaction-diffusion structure in SISO linear dynamical networks," in *Decision and Control (CDC), 2010 Proceedings of the 49th IEEE Conference on*. IEEE, 2010, pp. 5350–5355.
- [31] T. Ishizaki, K. Kashima, J. Imura, and K. Aihara, "Model order reduction for MIMO linear dynamical networks via reaction-diffusion transformation," in *American Control Conference (ACC), 2011*. IEEE, 2011, pp. 5019–5024.
- [32] —, "Reaction-diffusion clustering of single-input dynamical networks," in *Decision and Control and European Control Conference (CDC-ECC), 2011 50th IEEE Conference on*. IEEE, 2011, pp. 7837–7842.
- [33] —, "Model reduction of multi-input dynamical networks based on clusterwise controllability," in *American Control Conference (ACC), 2012*. IEEE, 2012, pp. 2301–2306.
- [34] A. Barrat, M. Barthélemy, and A. Vespignani, *Dynamical processes on complex networks*. Cambridge University Press, 2008.
- [35] L. Farina and S. Rinaldi, *Positive linear systems: Theory and applications*. Wiley-Interscience, 2011.
- [36] L. Benvenuti and L. Farina, "A tutorial on the positive realization problem," *Automatic Control, IEEE Transactions on*, vol. 49, no. 5, pp. 651–664, 2004.
- [37] J. H. Wilkinson, *The algebraic eigenvalue problem*. Oxford Univ Press, 1965, vol. 155.
- [38] B. Datta and K. Datta, "An algorithm to assign canonical forms by state feedback," in *Decision and Control, 1989., Proceedings of the 28th IEEE Conference on*. IEEE, 1989, pp. 2373–2374.
- [39] J. Lee, V. Balakrishnan, C.-K. Koh, and D. Jiao, "From $O(k^2N)$ to $O(N)$: A fast and high-capacity eigenvalue solver for full-wave extraction of very large scale on-chip interconnects," *IEEE Transactions on Microwave Theory and Techniques*, vol. 57, no. 12, p. 3219, 2009.
- [40] A. Rantzer, "Distributed control of positive systems," in *Decision and Control and European Control Conference (CDC-ECC), 2011 50th IEEE Conference on*. IEEE, 2011, pp. 6608–6611.
- [41] R. A. Horn and C. R. Johnson, *Matrix analysis*. Cambridge university press, 1990.
- [42] H. S. Stone, "An efficient parallel algorithm for the solution of a tridiagonal linear system of equations," *Journal of the ACM (JACM)*, vol. 20, no. 1, pp. 27–38, 1973.



Takayuki Ishizaki was born in Aichi, Japan, in 1985. He received the B.Sc., M.Sc., and Ph.D. degrees in engineering from Tokyo Institute of Technology, Tokyo, Japan, in 2008, 2009, and 2012, respectively.

He served as a Research Fellow of the Japan Society for the Promotion of Science from April 2011 to October 2012. From October to November 2011, he was a Visiting Student at Laboratoire Jean Kuntzmann, Université Joseph Fourier, Grenoble, France. From June to October 2012, he was a Visiting Researcher at School of Electrical Engineering, Royal Institute of Technology, Stockholm, Sweden. Since November 2012, he has been with the Department of Mechanical and Environmental Informatics, Graduate School of Information Science and Engineering, Tokyo Institute of Technology, where he is currently an Assistant Professor. His research interests include the development of model reduction and its applications.

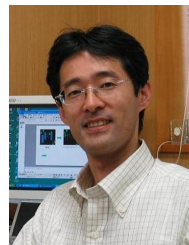
Dr. Ishizaki is a member of IEEE, SICE, and ISCIE. He was named as a finalist of the 51st CDC Best Student-Paper Award.



Kenji Kashima was born in 1977 in Oita, Japan. He received his B.Sc. degree in engineering and his M.Sc. and Ph.D. degrees in informatics from Kyoto University in 2000, 2002 and 2005, respectively.

He was an Assistant Professor of the Graduate School of Information Science and Engineering, Tokyo Institute of Technology from 2005 to 2011. From April 2010 to March 2011, he was at Universität Stuttgart, supported by the Alexander von Humboldt Foundation, Germany. Since 2011, he has been an Associate Professor of the Graduate School of Engineering Science, Osaka University.

He has served as an Associate Editor of the IEEE CSS Conference Editorial Board since 2011. His research interests include system and control theory for distributed and stochastic phenomena in large scale dynamical systems, as well as its applications.



Jun-ichi Imura (M'93) was born in Gifu, Japan, in 1964. He received the M.S. degree in applied systems science and the Ph.D. degree in mechanical engineering from Kyoto University, Kyoto, Japan, in 1990 and 1995, respectively.

He served as a Research Associate in the Department of Mechanical Engineering, Kyoto University, from 1992 to 1996, and as an Associate Professor in the Division of Machine Design Engineering, Faculty of Engineering, Hiroshima University, from 1996 to 2001. From May 1998 to April 1999, he was a Visiting Researcher at the Faculty of Mathematical Sciences, University of Twente, Enschede, The Netherlands. Since 2001, he has been with the Department of Mechanical and Environmental Informatics, Graduate School of Information Science and Engineering, Tokyo Institute of Technology, Tokyo, Japan, where he is currently a Professor. His research interests include modeling, analysis, and synthesis of nonlinear systems, hybrid systems, and large-scale network systems with applications to biological systems, industrial process systems, and robot intelligence. He is an Associate Editor of *Automatica* (2009-) and the *Nonlinear Analysis: Hybrid Systems* (2011-).

Dr. Imura is a member of IEEE, SICE, ISCIE, IEICE, and The Robotics Society of Japan.



Kazuyuki Aihara received the B.E. degree of electrical engineering in 1977 and the Ph.D. degree of electronic engineering 1982 from the University of Tokyo, Japan. Currently, he is Professor of Institute of Industrial Science, the University of Tokyo, Professor of Graduate School of Information Science and Technology, the University of Tokyo, Professor of Graduate School of Engineering, the University of Tokyo, and Director of Collaborative Research Center for Innovative Mathematical Modelling, the University of Tokyo.

His research interests include mathematical modeling of complex systems, parallel distributed processing with spatio-temporal chaos, and time series analysis of complex data.